Electronic Supplementary Material (ESI) for Physical Chemistry Chemical Physics.
This journal is © the Owner Societies 2023

Alkylphosphonium Carboxylate Ionic Liquids with Tuned Microscopic Structures and Properties

Nicolas Scaglione,[†] Jocasta Avila,[†] Eduards Bakis,[‡] Agilio Pádua,[†] and Margarida Costa Gomes*,[†]

[†]*Laboratoire de Chimie de l'ENS Lyon, CNRS and Université de Lyon, 46 allée d'Italie, 69364 Lyon, France*

[‡]*Faculty of Chemistry, University of Latvia, Jelgavas 1, Riga, LV-1004, Latvia.*

E-mail: margarida.costa-gomes@ens-lyon.fr

Supplementary Information

Ionic liquids synthesis and characterization

The concentration of $[P_{4,4,4,4}][OH]$ aqueous solution given by the supplier was 41.4 %. The $[P_{4,4,4,4}][RCOO]$ ILs were all synthesized *via* a neutralization reaction of $[P_{4,4,4,4}][OH]$ with the corresponding carboxylic acid of the $[RCOO]^-$ (Figure S1). The carboxylic acids were used without further purification based on the given purity.

General synthesis route of $[P_{4,4,4,4}][RCOO]$: An aqueous solution of $[P_{4,4,4,4}][OH]$ (1 eq) was introduced into a 100 mL round bottom flask, followed by the dropwise addition of a slight excess of the carboxylic acid (1.02 eq) under continuous stirring. The flask was initially placed in a water bath with ice during the addition, then, the mixture was stirred for 3 hours in a water bath at room temperature (r.t.). A slight increase in temperature was noticed upon addition of the acid into the aqueous solution. Then, acetonitrile (ACN) was added to the obtained solution in order to create an azeotrope (% mol ACN : H_2O = 69.26 : 30.74) to facilitate the removal of the water formed under reduced pressure at about 40 mbar and 323 K in a rotary evaporator. Thereafter, the obtained compound was dried either by freeze-drying if it was a liquid at r. t. or under vacuum (1×10^{-4} bar) at a temperature above its melting point. The synthesis was realised on a 5 to 50 mmol scale and the ILs were obtained with a minimum yield of 95 %.

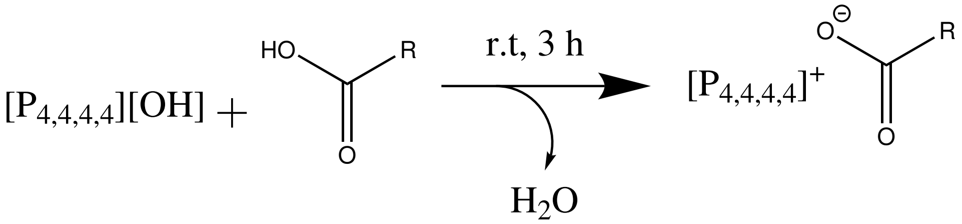

Figure S1 – Scheme of the neutralization reaction of the tetrabutylphosphonium hydroxide ($[P_{4,4,4,4}][OH]$) by the carboxylic acid (RCOOH) to produce the corresponding IL $[P_{4,4,4,4}][RCOO]$.

Tetrabutylphosphonium acetate $[P_{4,4,4,4}][C_1COO]$ was synthesized and characterized as already described in our previous work.[1]

Tetrabutylphosphonium isovalerate $[P_{4,4,4,4}][MeC_3COO]$, the colourless viscous liquid obtained from the rotary evaporator was dried under vacuum (1×10^{-4} bar) at 343 K under stirring (400 rpm). After the water removal, a white solid was obtained.

^{1}H NMR (400 MHz, C_6D_6, 343 K) δ: 0.91 (d, 6H, $^3J_{HH}$ = 6.4 Hz, $(\mathbf{CH_3})_2CHCH_2COO$); 0.96

(t, 12H, $^3J_{HH} = 7.3$ Hz, $P(CH_2CH_2CH_2C\mathbf{H_3})_4$); 1.50 (m, 8H, $P(CH_2CH_2C\mathbf{H_2}CH_3)_4$); 1.60 (m, 8H, $P(CH_2C\mathbf{H_2}CH_2CH_3)_4$); 1.88 (m, 2H, $(CH_3)_2CHC\mathbf{H_2}COO$); 2.01 (m, 1H, $(CH_3)_2C\mathbf{H}CH_2COO$); 2.63 (m, 8H, $P(C\mathbf{H_2}CH_2CH_2CH_3)_4$) ppm. ^{13}C NMR (100 MHz, C_6D_6, 298 K) δ: 13.76 (4C, $P(CH_2CH_2CH_2\mathbf{C}H_3)_4$); 19.21 (4C, $P(\mathbf{C}H_2CH_2CH_2CH_3)_4$); 23.69 (2C, $(\mathbf{C}H_3)_2CHCH_2COO$); 24.20 – 24.58 (8C, $P(CH_2\mathbf{C}H_2\mathbf{C}H_2CH_3)_4$); 26.87 (1C, $(CH_3)_2\mathbf{C}HCH_2COO$); 49.35 (1C, $(CH_3)_2CH\mathbf{C}H_2COO$); 175.00 (1C, $(CH_3)_2CHCH_2\mathbf{C}OO$) ppm. ^{31}P NMR (161 MHz, C_6D_6, 298 K) δ: 33.83 (1P, $\mathbf{P}(CH_2CH_2CH_2CH_3)_4$) ppm. ν (cm^{-1}): 2960; 2932; 2874; 2863; 1575; 1466; 1448; 1419; 1362; 1316; 1249; 1210; 1166; 1096; 1002; 970; 908; 884; 833; 817; 723.5. MS ES^+ m/z (% Rel. Intensity): 259 (100, $[P_{4,4,4,4}]^+$). MS ES^- m/z (% Rel. Intensity): 101 (100, $[MeC_3COO]^-$).

Tetrabutylphosphonium 2,2,4,4-tetramethylpentanoate $\mathbf{[P_{4,4,4,4}][Me_4C_4COO]}$, the colorless viscous liquid obtained from the rotary evaporator was dried under vacuum (1×10^{-4} bar) at 323 K under stirring (400 rpm). The product was collected as a colourless viscous liquid.

^1H NMR (400 MHz, C_6D_6, 343 K) δ: 0.92 – 1.00 (m, 21H, $(C\mathbf{H_3})_3CCH_2C(CH_3)_2COO$ + $P(CH_2CH_2CH_2C\mathbf{H_3})_4$); 1.07 (s, 6H, $(CH_3)_3CCH_2C(C\mathbf{H_3})_2COO$); 1.50 (m, 8H, $P(CH_2CH_2C\mathbf{H_2}CH_3)_4$); 1.55 (s, 2H, $(CH_3)_3CC\mathbf{H_2}C(CH_3)_2COO$); 1.59 (m, 8H, $P(CH_2C\mathbf{H_2}CH_2CH_3)_4$); 2.71 (m, 8H, $P(C\mathbf{H_2}CH_2CH_2CH_3)_4$) ppm. ^{13}C NMR (100 MHz, C_6D_6, 343 K) δ: 14.21 (4C, $P(CH_2CH_2CH_2\mathbf{C}H_3)_4$); 19.62 (4C, $P(\mathbf{C}H_2CH_2CH_2CH_3)_4$); 24.60 – 24.97 (8C, $P(CH_2\mathbf{C}H_2\mathbf{C}H_2CH_3)_4$); 30.85 (2C, $(CH_3)_3CCH_2C(\mathbf{C}H_3)_2COO$); 32.29 (3C, $(\mathbf{C}H_3)_3CCH_2C(CH_3)_2COO$); 32.55 (1C, $(CH_3)_3\mathbf{C}CH_2C(CH_3)_2COO$); 43.60 (1C, $(CH_3)_3CCH_2\mathbf{C}(CH_3)_2COO$);
57.72 (1C, $(CH_3)_3C\mathbf{C}H_2C(CH_3)_2COO$) 180.28 (1C, $(CH_3)_3CCH_2C(CH_3)_2\mathbf{C}OO$) ppm. ^{31}P NMR (161 MHz, C_6D_6, 343 K) δ: 33.76 (1P, $\mathbf{P}(CH_2CH_2CH_2CH_3)_4$) ppm. ν (cm^{-1}): 2958; 2934; 2906; 2872; 1569; 1476; 1466; 1423; 1394; 1385; 1359; 1346; 1310; 1241; 1226; 1099; 1005; 970; 942; 919; 907; 882; 849; 801; 797; 749; 719; 598. MS ES^+ m/z (% Rel. Intensity): 259 (100, $[P_{4,4,4,4}]^+$). MS ES^- m/z (% Rel. Intensity): 157 (100, $[Me_4C_4COO]^-$).

Trihexyltetradecylphosphonium 2,2,4,4-tetramethylpentanoate $\mathbf{[P_{6,6,6,14}][Me_4C_4COO]}$, potassium 2,2,4,4-tetramethylpentanoate (Me_4C_4COOK) was prepared by dissolving stoichiometric quantities of 2,2,4,4-tetramethylpentanoic acid (1 eq) and anhydrous potassium carbonate (2 eq) in methanol, and evaporating the solution to dryness via rotary evaporation at 60 °C. The salt was dried at 80 °C and 10^{-2} mbar for 24 h prior to use. Using the analytical balance,

$[P_{6,6,6,14}][Cl]$ (13.4292 g, 25.8597 mmol, 1 eq) and the potassium salt of 2,2,4,4-tetramethylpentanoic acid (5.0748 g, 25.8485 mmol, 0.9996 eq) were weighed in a flask and combined with ethyl acetate (100 mL). The suspension was stirred at ambient temperature for 24 h. The solids were separated via centrifugation (20 min, 6000 rpm). The solution was evaporated using the rotary evaporator, and the viscous residue stirred at high vacuum (45 °C, 24 h). The brownish viscous liquid was dissolved in ethyl acetate (250 mL) and saturated with small portions of water until two phases persisted after shaking (4 x 3 mL). The mixture was further diluted with ethyl acetate (100 mL), well shaken and left to phase-separate. The aqueous phase was removed, and further extractions with water performed (10 x 3 mL). Between extractions at least 20 min were observed to allow efficient phase separation. After the final extraction the mixture was left to phase-separate overnight, and the clear organic phase evaporated via rotary evaporator (60 °C). Distillation of a cloudy ethyl acetate-water mixture could be observed. In order to further dry the ionic liquid, it was dissolved in benzene (10 mL) and the solvent evaporated at reduced pressure (200 mbar). Finally, the drying with the rotary evaporator was continued at 17 mbar until no more bubbling was observed. Further drying at high vacuum (45 °C, 24 h) provided a viscous brown liquid with a characteristic sweet odour (13.2737 g, 80 %).

^{1}H NMR (400 MHz, C_6D_6, 343 K) δ: 0.89 – 0.98 (m, 12H, $P((CH_2)_5C\mathbf{H}_3)_3((CH_2)_{13}C\mathbf{H}_3))$; 1.01 (s, 9H, $(C\mathbf{H}_3)_3CCH_2C(CH_3)_2COO)$; 1.13 (s, 6H, $(CH_3)_3CCH_2C(C\mathbf{H}_3)_2COO)$; 1.27 – 1.45 (m, 32H, $P(CH_2CH_2CH_2C\mathbf{H}_2C\mathbf{H}_2CH_3)_3(CH_2CH_2CH_2(C\mathbf{H}_2)_{10}CH_3))$; 1.51 (m, 8H, $P(CH_2CH_2C\mathbf{H}_2CH_2CH_2CH_3)_3(CH_2CH_2C\mathbf{H}_2(CH_2)_{10}CH_3))$; 1.61 (s, 2H, $(CH_3)_3CC\mathbf{H}_2C(CH_3)_2COO)$; 1.65 (m, 8H, $P(CH_2C\mathbf{H}_2CH_2CH_2CH_2CH_3)_3(CH_2C\mathbf{H}_2(CH_2)_{11}CH_3))$; 2.76 (m, 8H, $P(C\mathbf{H}_2(CH_2)_4CH_3)_3(C\mathbf{H}_2(CH_2)_{12}CH_3))$ ppm. ^{13}C NMR (100 MHz, C_6D_6, 343 K) δ: 14.29 (3C, $P(CH_2(CH_2)_4\mathbf{C}H_3)_3(CH_2(CH_2)_{12}CH_3))$; 14.67 (3C, $P(CH_2(CH_2)_4CH_3)_3(CH_2(CH_2)_{12}\mathbf{C}H_3))$; 22.37 – 22.67 (5C, $P(CH_2\mathbf{C}H_2(CH_2)_3CH_3)_3(CH_2\mathbf{C}H_2(CH_2)_{11}CH_3) + (CH_3)_3C\mathbf{C}H_2C(CH_3)_2COO)$; 22.85, 23.02, 29.52, 29.72, 29.90, 30.03, 30.08, 31.13, 31.47, 31.71, (24C, $P((CH_2)_2(\mathbf{C}H_2)_3CH_3)_3((CH_2)_2(\mathbf{C}H_2)_{11}CH_3))$; 19.64 (4C, $P(\mathbf{C}H_2CH_2CH_2CH_3)_4)$; 23.11 – 23.39 (8C, $P(\mathbf{C}H_2\mathbf{C}H_2CH_2CH_2CH_2CH_3)_3(CH_2\mathbf{C}H_2\mathbf{C}H_2(CH_2)_{10}CH_3))$; 30.22 (2C, $(CH_3)_3CCH_2C(\mathbf{C}H_3)_2COO)$; 31.98 (3C, $(\mathbf{C}H_3)_3CCH_2C(CH_3)_2COO)$; 32.30 (1C, $(CH_3)_3\mathbf{C}CH_2C(CH_3)_2COO)$; 43.24 (1C, $(CH_3)_3CCH_2\mathbf{C}(CH_3)_2COO)$; 55.19 (1C, $(CH_3)_3C\mathbf{C}H_2C(CH_3)_2COO)$ 180.37 (1C, $(CH_3)_3CCH_2C(CH_3)_2\mathbf{C}OO)$

ppm. ^{31}P NMR (161 MHz, C_6D_6, 343 K) δ: 33.73 (1P, $\mathbf{P}((CH_2)_5CH_3)_3((CH_2)_{13}CH_3))$ ppm. ν (cm^{-1}): 2954; 2924; 2874; 2855; 1568; 1481; 1466; 1395; 1386; 1367; 1359; 1345; 1310: 1266; 1248; 1223; 1181; 1112; 1023; 980; 917; 888; 851; 801; 775; 720; 602; 597; 580; 572; 556. MS ES$^+$ m/z (% Rel. Intensity): 483.5 (100, $[P_{6,6,6,14}]^+$). MS ES$^-$ m/z (% Rel. Intensity): 157 (100, $[Me_4C_4COO]^-$).

Tetrabutylphosphonium hexanoate $[\mathbf{P_{4,4,4,4}}][\mathbf{C_5COO}]$, the colorless liquid obtained from the rotary evaporator was dried under vacuum (1×10^{-4} bar) at 323 K under stirring (400 rpm). The product was collected as a colourless viscous liquid.

^{1}H NMR (400 MHz, C_6D_6, 343 K) δ: 0.92 (t, 3H, $^3J_{HH}$ = 7.0 Hz, $\mathbf{CH_3}(CH_2)_3CH_2COO$); 1.00 (t, 12H, $^3J_{HH}$ = 7.4 Hz, $P(CH_2CH_2CH_2C\mathbf{H_3})_4$); 1.33 (m, 6H, $CH_3(C\mathbf{H}_2)_3CH_2COO$); 1.54 (m, 8H,$P(CH_2CH_2C\mathbf{H_2}CH_3)_4$); 1.64 (m, 8H,$P(CH_2C\mathbf{H}_2CH_2CH_3)_4$); 1.97 (t, 2H, $^3J_{HH}$ = 7.4 Hz, $CH_3(CH_2)_3C\mathbf{H}_2COO$); 2.68 (m, 8H, $P(C\mathbf{H_2}CH_2CH_2CH_3)_4$) ppm. ^{13}C NMR (100 MHz, C_6D_6, 343 K) δ: 13.82 (4C, $P(CH_2CH_2CH_2\mathbf{C}H_3)_4$); 14.42 (1C, $\mathbf{C}H_3(CH_2)_3CH_2COO$) ; 19.07 (4C, $P(\mathbf{C}H_2CH_2CH_2CH_3)_4$); 23.24 (1C, $CH_3\mathbf{C}H_2(CH_2)_2CH_2COO$); 24.40 (4C, $P(CH_2\mathbf{C}H_2CH_2CH_3)_4$); 24.55 (4C, $P(CH_2CH_2\mathbf{C}H_2CH_3)_4$); 27.58 (1C, $CH_3CH_2\mathbf{C}H_2CH_2CH_2COO$); 33.09 (1C, $CH_3(CH_2)_2\mathbf{C}H_2CH_2COO$; 38.60 (1C, $CH_3(CH_2)_3\mathbf{C}H_2COO$); 175.47 (1C, $CH_3(CH_2)_3CH_2\mathbf{C}OO$) ppm. ^{31}P NMR (161 MHz, C_6D_6, 343 K) δ: 33.81 (1P, $\mathbf{P}(CH_2CH_2CH_2CH_3)_4$) ppm. ν (cm^{-1}): 2956; 2930; 2872; 2851; 1564; 1466; 1429; 1411; 1382; 1343; 1313; 1288; 1232; 1190; 1098; 1053; 1005; 969; 921; 908; 811; 849; 755; 724. MS ES$^+$ m/z (% Rel. Intensity): 259 (100, $[P_{4,4,4,4}]^+$). MS ES$^-$ m/z (% Rel. Intensity): 115 (100, $[C_5COO]^-$).

Tetrabutylphosphonium dodecanoate $[\mathbf{P_{4,4,4,4}}][\mathbf{C_{11}COO}]$, the colorless liquid obtained from the rotary evaporator was dried under vacuum (1×10^{-4} bar) at 323 K under stirring (400 rpm). The product was collected as a colourless viscous liquid.

^{1}H NMR (400 MHz, C_6D_6, 343 K) δ: 0.91 (t, 3H, $^3J_{HH}$ = 6.6 Hz, $C\mathbf{H}_3(CH_2)_9CH_2COO$); 0.98 (t, 12H, $^3J_{HH}$ = 7.3 Hz, $P(CH_2CH_2CH_2C\mathbf{H_3})_4$); 1.30 (m, 16H, $CH_3CH_2(C\mathbf{H}_2)_8CH_2COO$); 1.52 (m, 8H, $P(CH_2CH_2C\mathbf{H_2}CH_3)_4$); 1.54 (m, 2H, $CH_3(CH_2)_8C\mathbf{H}_2CH_2COO$); 1.61 (m, 8H, $P(CH_2C\mathbf{H_2}CH_2CH_3)_4$); 1.96 (t, 2H, $^3J_{HH}$ = 7.4 Hz, $CH_3(CH_2)_9C\mathbf{H}_2COO$); 2.65 (m, 8H, $P(C\mathbf{H_2}CH_2CH_2CH_3)_4$) ppm. ^{13}C NMR (100 MHz, C_6D_6, 343 K) δ: 13.77 (4C, $P(CH_2CH_2CH_2\mathbf{C}H_3)_4$); 14.23 (1C, $\mathbf{C}H_3(CH_2)_9CH_2COO$); 19.24 (4C, $P(\mathbf{C}H_2CH_2CH_2CH_3)_4$); 22.97 (1C, $CH_3\mathbf{C}H_2(CH_2)_8CH_2COO$);

24.31 – 24.57 (8C, P(CH$_2$**C**H$_2$**C**H$_2$CH$_3$)$_4$); 27.82 (1C, CH$_3$(CH$_2$)$_8$**C**H$_2$CH$_2$COO); 29.63 – 32.30 (8C, CH$_3$CH$_2$(**C**H$_2$)$_8$CH$_2$COO); 39.78 (1C, CH$_3$(CH$_2$)$_9$**C**H$_2$COO); 175.58 (1C, CH$_3$(CH$_2$)$_9$CH$_2$**C**OO) ppm. ^{31}P NMR (161 MHz, C$_6$D$_6$, 298 K) δ: 33.71 (1P, **P**(CH$_2$CH$_2$CH$_2$CH$_3$)$_4$) ppm. ν (cm^{-1}): 2958; 2923; 2872; 2854; 1576; 1466; 1418; 1377; 1306; 1238; 1098; 1042; 1005; 969; 919; 908; 811; 752; 721. MS ES$^+$ m/z (% Rel. Intensity): 259 (100, [P$_{4,4,4,4}$]$^+$). MS ES$^-$ m/z (% Rel. Intensity): 199 (100, [C$_{11}$COO]$^-$).

Trihexyltetradecylphosphonium dodecanoate [P$_{6,6,6,14}$][C$_{11}$COO] synthesis began with the formation of potassium dodecanoate (C$_{11}$COOK). To the suspension of a finely ground potassium carbonate K$_2$CO$_3$ (10.46 g, 75.68 mol, 1.000 eq) in 96 % ethanol (550 mL), dodecanoic acid was added (30.90 g, 154.28 mol, 2.038 eq), and the mixture stirred under reflux for 12 h. The clear solution was allowed to cool to ambient temperature and then cooled to 5 °C in a fridge. The crystals were collected *via* suction filtration and washed on the filter with ethanol (2 °C, 2 x 50 mL) and petroleum ether (1 x 50 mL). The product was dried in air and then at reduced pressure (0.1 mbar, 80 °C, 24 h) providing white scaly flakes (22.02 g, 61 %).

Thereafter, the trihexyltetradecylphosphonium chloride (10.1566 g, 19.557 mol, 1.000 eq) and potassium dodecanoate (4.6627 g, 19.5575 mol, 1.000 eq) were mixed together and combined with 2-methyltetrahydrofuran (60 mL). After a vigorous stirring (60 °C, 15 min) water was added (10 mL) and the stirring continued for 3 h without additional heating. The solution was cooled to 5 °C and the aqueous (lower) layer removed. The organic layer was further washed with water by vigorous stirring (3 x 10 mL, 30 min per wash), and further in a separatory funnel (3 x 10 mL). The absence of halide ions in washings was checked with the AgCl test by taking 1 mL of the aqueous phase, adding 6 drops of 70 % HNO$_3$, shaking the mixture with 1 mL of CHCl$_3$, and treating the aqueous phase with 0.5 mL of 0.10 M aqueous AgNO$_3$. In 5 min the solution was visually inspected for cloudiness. The washing was assumed to be complete when the level of cloudiness no longer reduced for further washings. The slightly yellow-brown organic phase was filtered through the hydrophobic filter paper, and the solution was briefly warmed up to 60 °C with a small amount of powdered activated charcoal. The mixture was cooled in an ice bath, filtered via gravity, followed by a 40 µm PTFE membrane filter. No significant decolouration of the solution was achieved. The solvent was removed via rotary evaporation at reduced pressure (60 °C, 4 mbar) providing a viscous orange liquid (10.56 g, 79.0 %). Further stirred drying (50 °C, 0.1 mbar, 24 h) caused darkening of the liquid without changes in spectroscopic data.

^{1}H NMR (400 MHz, C_6D_6, 343 K) δ: 0.90 – 1.02 (m, 15H, $C\mathbf{H}_3(CH_2)_9CH_2COO$ + $P((CH_2)_5C\mathbf{H}_3)_3((CH_2)_{13}C\mathbf{H}_3)$); 1.32 – 1.45 (m, 16H, $CH_3(C\mathbf{H}_2)_8CH_2CH_2COO$ + $P((CH_2)_3(C\mathbf{H}_2)_2CH_3)((CH_2)_3(C\mathbf{H}_2)_{10}CH_3)$); 1.54 (m, 8H, $P((CH_2)_2C\mathbf{H}_2(CH_2)_2CH_3)_3((CH_2)_2C\mathbf{H}_2(CH_2)_{10}CH_3)$); 1.60 (m, 2H, $CH_3(CH_2)_8C\mathbf{H}_2CH_2COO$); 1.67 (m, 8H, $P(CH_2C\mathbf{H}_2(CH_2)_3CH_3)_3(CH_2C\mathbf{H}_2(CH_2)_{11}CH_3)$); 2.04 (t, 2H, $^{3}J_{HH} = 7.2$ Hz, $CH_3(CH_2)_9C\mathbf{H}_2COO$); 2.71 (m, 8H, $P(C\mathbf{H}_2(CH_2)_4CH_3)_3(C\mathbf{H}_2(CH_2)_{12}CH_3)$) ppm. ^{13}C NMR (100 MHz, C_6D_6, 343 K) δ: 14.31 (5C, $P((CH_2)_{13}\mathbf{C}H_3)_3((CH_2)_5\mathbf{C}H_3)$ + $\mathbf{C}H_3(CH_2)_9CH_2COO$); 19.50 (4C, $P(\mathbf{C}H_2(CH_2)_4CH_3)_3(\mathbf{C}H_2(CH_2)_{12}CH_3)$); 22.40 (4C, $P(CH_2\mathbf{C}H_2(CH_2)_3CH_3)_3(CH_2\mathbf{C}H_2(CH_2)_{11}CH_3)$); 22.90, 23.06, 29.49 – 32.52 (24C, $P((CH_2)_3(\mathbf{C}H_2)_2CH_3)_3((CH_2)_3(\mathbf{C}H_2)_{10}CH_3)$ + $CH_3CH_2(\mathbf{C}H_2)_8CH_2COO$); 27.69 (1C, $CH_3(CH_2)_8\mathbf{C}H_2CH_2COO$); 31.10 (4C, $P((CH_2)_2\mathbf{C}H_2(CH_2)_2CH_3)_3((CH_2)_2\mathbf{C}H_2(CH_2)_{10}CH_3)$); 39.34 (1C, $CH_3(CH_2)_9\mathbf{C}H_2COO$); 176.04 (1C, $CH_3(CH_2)_9CH_2\mathbf{C}OO$) ppm. ^{31}P NMR (161 MHz, C_6D_6, 298 K) δ: 33.50 (1P, $\mathbf{P}((CH_2)_5CH_3)_3((CH_2)_{13}CH_3)$) ppm. ν (cm^{-1}): 2955; 2922; 2874; 2853; 1576; 1466; 1416; 1378; 1302; 1216; 1111; 989; 861; 807; 751; 721; 577. MS ES^{+} m/z (% Rel. Intensity): 483.5 (100, $[P_{6,6,6,14}]^{+}$). MS ES^{-} m/z (% Rel. Intensity): 199 (100, $[C_{11}COO]^{-}$).

Tetrabutylphosphonium cyclohexanecarboxylate $[\mathbf{P_{4,4,4,4}}][\mathbf{c{-}C_6COO}]$, the colorless liquid obtained from the rotary evaporator was dried under vacuum (1×10^{-4} bar) at 343 K under stirring (400 rpm). After the water removal, a white solid was obtained.

^{1}H NMR (400 MHz, C_6D_6, 343 K) δ: 0.96 (t, 12H, $^{3}J_{HH} = 7.2$ Hz, $P(CH_2CH_2CH_2C\mathbf{H_3})_4$); 1.20 (m, 1H, $(C\mathbf{H_{ax}}H_{eq})(CH_2)_2(CH_2)_2CHCOO$); 1.23 (m, 2H, $CH_2(C\mathbf{H_{ax}}H_{eq})_2(CH_2)_2CHCOO$); 1.39 (m, 2H, $CH_2(CH_2)_2(C\mathbf{H_{ax}}H_{eq})_2CHCOO$); 1.49 (m, 8H, $P(CH_2CH_2C\mathbf{H_2}CH_3)_4$); 1.57 (m, 1H, $(CH_{ax}\mathbf{H_{eq}})(CH_2)_2(CH_2)_2CHCOO$); 1.59 (m, 8H, $P(CH_2C\mathbf{H_2}CH_2CH_3)_4$); 1.66 (m, 2H, $CH_2(CH_{ax}\mathbf{H_{eq}})_2(CH_2)_2CHCOO$); 1.82 (m, 2H, $CH_2(CH_2)_2(CH_{ax}\mathbf{H_{eq}})_2CHCOO$); 1.92 (m, 1H, $CH_2(CH_2)_2(CH_2)_2C\mathbf{H}COO$); 2.60 (m, 8H, $P(C\mathbf{H_2}CH_2CH_2CH_3)_4$) ppm. ^{13}C NMR (100 MHz, C_6D_6, 343 K) δ: 13.70 (4C, $P(CH_2CH_2CH_2\mathbf{C}H_3)_4$); 19.22 (4C, $P(\mathbf{C}H_2CH_2CH_2CH_3)_4$); 24.14 – 24.45 (8C, $P(CH_2\mathbf{C}H_2\mathbf{C}H_2CH_3)_4$); 26.99 (2C, $CH_2(\mathbf{C}H_2)_2(CH_2)_2CHCOO$); 27.38 (1C, $\mathbf{C}H_2(CH_2)_2(CH_2)_2CHCOO$); 31.49 (2C, $CH_2(CH_2)_2(\mathbf{C}H_2)_2CHCOO$); 47.23 (1C, $CH_2(CH_2)_2(CH_2)_2\mathbf{C}HCOO$);

178.13 (2C, $CH_2(CH_2)_2(CH_2)_2CH\mathbf{C}OO$) ppm. ^{31}P NMR (161 MHz, C_6D_6, 343 K) δ: 33.62 (1P, $\mathbf{P}(CH_2CH_2CH_2CH_3)_4$) ppm. ν (cm^{-1}): 2959; 2922; 2873; 2849; 1570; 1465; 1447; 1419; 1369; 1346; 1326; 1285; 1274; 1235; 1212; 1135; 1094; 1055; 1005; 968; 921; 909; 893; 887; 833; 813; 799; 764; 751; 721; 657. MS ES$^+$ m/z (% Rel. Intensity): 259 (100, $[P_{4,4,4,4}]^+$). MS ES$^-$ m/z (% Rel. Intensity): 127 (100, $[c{-}C_6COO]^-$).

Tetrabutylphosphonium phenylacetate $[\mathbf{P_{4,4,4,4}}][\mathbf{PhC_1COO}]$, the colourless liquid obtained from the rotary evaporator was dried under vacuum (1×10^{-4} bar) at 343 K under stirring (400 rpm). After the water removal, a white solid was obtained.

^{1}H NMR (400 MHz, DMSO-d_6, 343 K) δ: 0.95 (t, 12H, $^3J_{HH}$ = 7.2 Hz, $P(CH_2CH_2CH_2C\mathbf{H_3})_4$); 1.44 (m, 16H, $P(CH_2C\mathbf{H_2}C\mathbf{H_2}CH_3)_4$); 2.40 (m, 8H, $P(C\mathbf{H_2}CH_2CH_2CH_3)_4$); 3.30 (s, 2H, $PhC\mathbf{H_2}COO$; 7.16 (m, 1H, $C\mathbf{H}(CH)_2(CH)_2CCH_2COO$); 7.34 (m, 4H, $CH(C\mathbf{H})_2(C\mathbf{H})_2CCH_2COO$) ppm. ^{13}C NMR (100 MHz, DMSO-d_6, 343 K) δ: 12.35 (4C, $P(CH_2CH_2CH_2\mathbf{C}H_3)_4$); 17.28 (4C, $P(\mathbf{C}H_2CH_2CH_2CH_3)_4$); 22.56 (4C, $P(CH_2CH_2\mathbf{C}H_2CH_3)_4$); 22.79 (4C, $P(CH_2\mathbf{C}H_2CH_2CH_3)_4$); 46.84 (1C $Ph\mathbf{C}H_2COO$); 123.23 (1C, $\mathbf{C}H(CH)_2(CH)_2CCH_2COO$);
126.12 (2C, $CH(\mathbf{C}H)_2(CH)_2CCH_2COO$); 128.33 (2C, $CH(CH)_2(\mathbf{C}H)_2CCH_2COO$); 140.97 (1C, $CH(CH)_2(CH)_2\mathbf{C}CH_2COO$); 170.86 ($PhCH_2\mathbf{C}OO$) ppm. ^{31}P NMR (161 MHz, DMSO-d_6, 343 K) δ: 33.59 (1P, $\mathbf{P}(CH_2CH_2CH_2CH_3)_4$) ppm. ν (cm^{-1}): 3086; 3062; 3029; 2958; 2932; 2872; 1713; 1658; 1602; 1496; 1465; 1454; 1413; 1380; 1160; 1139; 1098; 1075; 1051; 1031; 1004; 968; 918; 646; 599; 589; 570; 564. MS ES$^+$ m/z (% Rel. Intensity): 259 (100, $[P_{4,4,4,4}]^+$). MS ES$^-$ m/z (% Rel. Intensity): 135 (100, $[PhC_1COO]^-$).

Tetrabutylphosphonium *p*-methylbenzoate $[\mathbf{P_{4,4,4,4}}][$*p*$-\mathbf{MeBzCOO}]$, the colorless liquid obtained from the rotary evaporator was dried under vacuum (1×10^{-4} bar) at 363 K under stirring (400 rpm). After the water removal, a white solid was obtained.

^{1}H NMR (400 MHz, DMSO-d_6, 343 K) δ: 0.99 (t, 12H, $^3J_{HH}$ = 7.1 Hz, $P(CH_2CH_2CH_2C\mathbf{H_3})_4$); 1.50 (m, 8H, $P(CH_2CH_2C\mathbf{H_2}CH_3)_4$); 1.59 (m, 8H, $P(CH_2C\mathbf{H_2}CH_2CH_3)_4$); 2.27 (m, 8H, $P(C\mathbf{H_2}CH_2CH_2CH_3)_4$); 2.37 (s, 3H, $C\mathbf{H_3}PhCOO$; 7.11 (d, 2H, $^3J_{HH}$ = 7.9 Hz, $CH_3C(CH)_2(C\mathbf{H})_2CCOO$); 7.94 (d, 2H, $^3J_{HH}$ = 7.7 Hz, $CH_3C(C\mathbf{H})_2(CH)_2CCOO$) ppm. ^{13}C NMR (100 MHz, DMSO-d_6, 343 K) δ: 12.85 ($P(CH_2CH_2CH_2\mathbf{C}H_3)_4$); 17.59 ($P(\mathbf{C}H_2CH_2CH_2CH_3)_4$); 19.98 ($\mathbf{C}H_3C(CH)_2(CH)_2CCOO$); 22.49 ($P(CH_2CH_2\mathbf{C}H_2CH_3)_4$); 22.71 ($P(CH_2\mathbf{C}H_2CH_2CH_3)_4$); 126.97 ($CH_3C(CH)_2(\mathbf{C}H)_2CCOO$)

; 128.66 ($CH_3C(\mathbf{C}H)_2(CH)_2CCOO$); 136.54 ($CH_3\mathbf{C}(CH)_2(CH)_2CCOO$); 137.69 ($CH_3C(CH)_2(CH)_2\mathbf{C}COO$); 168.72 ($CH_3C(CH)_2(CH)_2C\mathbf{C}OO$) ppm. ^{31}P NMR (161 MHz, DMSO-d_6, 343 K) δ: 33.81 (s, $\mathbf{P}(CH_2CH_2CH_2CH_3)_4$) ppm. ν (cm^{-1}):2958; 2931; 2893; 2873; 2730; 1602; 1562; 1465; 1458; 1351; 1230; 1167; 1099; 1092; 1067; 1019; 1005; 971; 918; 911; 897; 855; 838; 824; 813; 769; 752; 732; 720; 693 ; 640; 606. MS ES$^+$ m/z (% Rel. Intensity): 259 (100, [$P_{4,4,4,4}$]$^+$). MS ES$^-$ m/z (% Rel. Intensity): 135 (100, $p-$[MeBzCOO]$^-$).

Tetrabutylphosphonium 1H-tetrazole-1-acetate [$P_{4,4,4,4}$][TetrazC$_1$COO], the colorless viscous liquid obtained from the rotary evaporator was dried under vacuum (1×10^{-4} bar) at 323 K under stirring (400 rpm). After the water removal, a colorless liquid was collected. ^{1}H NMR (400 MHz, C_6D_6, 343 K) δ: 0.84 (t, 12H, $^3J_{HH} = 7.3$ Hz, $P(CH_2CH_2CH_2C\mathbf{H_3})_4$); 1.38 (m, 8H, $P(CH_2CH_2C\mathbf{H_2}CH_3)_4$); 1.49 (m, 8H, $P(CH_2C\mathbf{H_2}CH_2CH_3)_4$); 2.33 (m, 8H, $P(C\mathbf{H_2}CH_2CH_2CH_3)_4$); 4.73 (s, 2H, Tetraz$C\mathbf{H_2}COO$; 9.40 (s, 1H, $(N_3C\mathbf{H}N)CH_2CCOO$) ppm. ^{13}C NMR (100 MHz, C_6D_6, 343 K) δ: 14.21 ($P(CH_2CH_2CH_2\mathbf{C}H_3)_4$); 19.36 ($P(\mathbf{C}H_2CH_2CH_2CH_3)_4$); 24.45 ($P(CH_2\mathbf{C}H_2CH_2CH_3)_4$); 24.72 ($P(CH_2CH_2\mathbf{C}H_2CH_3)_4$); 53.19 (Tetraz$\mathbf{C}H_2CCOO$); 145.85 ($(N_3\mathbf{C}HN)CH_2CCOO$) ; 166.65 (Tetraz$CH_2\mathbf{C}COO$) ppm. ^{31}P NMR (161 MHz, C_6D_6, 343 K) δ: 33.66 (s, $\mathbf{P}(CH_2CH_2CH_2CH_3)_4$) ppm. ν (cm^{-1}): 3081; 2958; 2932; 2908; 2872; 1635; 1486; 1466; 1413; 1380; 1352; 1297; 1241; 1169; 1143; 1102; 1053; 1028; 1006; 970; 923; 908; 820; 795; 749; 721; 684; 658; 568. MS ES$^+$ m/z (% Rel. Intensity): 259 (100, [$P_{4,4,4,4}$]$^+$). MS ES$^-$ m/z (% Rel. Intensity): 127 (100, [TetrazC$_1$COO]$^-$).

Density and viscosity data

Table S1 – Experimental densities and molar volumes of the neat ILs and a few mixtures in the temperature range of 293–363 K. The deviations (δ) reported are relative to the fitting polynomials with coefficients listed in Table S2 and Table S3.

$\frac{T}{\mathrm{K}}$	$\frac{\rho}{\mathrm{g\,cm^{-3}}}$	$\frac{\delta}{\%}$	$\frac{V_m}{\mathrm{cm^3\,mol^{-1}}}$	$\frac{\delta}{\%}$	$\frac{T}{\mathrm{K}}$	$\frac{\rho}{\mathrm{g\,cm^{-3}}}$	$\frac{\delta}{\%}$	$\frac{V_m}{\mathrm{cm^3\,mol^{-1}}}$	$\frac{\delta}{\%}$
$[P_{4,4,4,4}][C_1COO]$					$[P_{4,4,4,4}][MeC_3COO]$				
303.148	0.935729	0.003	340.35	0.018	-	-	-	-	-
313.148	0.929771	0.001	342.54	0.001	-	-	-	-	-
323.148	0.923802	0.002	344.75	0.010	323.146	0.903840	0.004	398.93	0.009
333.148	0.917847	0.003	346.99	0.013	333.146	0.897580	0.003	401.71	0.0008
343.150	0.911917	0.002	349.24	0.010	343.154	0.891380	0.001	404.51	0.005
353.148	0.905997	0.001	352.24	0.001	353.154	0.885180	0.0009	407.34	0.001
363.151	0.900088	0.004	353.83	0.017	363.154	0.879013	0.003	410.20	0.009
$[P_{4,4,4,4}][Me_4C_4COO]$					$[P_{6,6,6,14}][Me_4C_4COO]$				
293.150	0.912674	0.01	456.53	0.008	293.149	0.886239	0.009	723.42	0.01
298.152	0.909638	0.008	458.05	0.004	298.152	0.883265	0.003	725.85	0.009
303.152	0.906614	0.0006	459.58	0.001	303.152	0.880298	0.0007	728.30	0.001
313.152	0.900615	0.01	462.64	0.003	313.152	0.874391	0.006	733.22	0.009
323.152	0.894696	0.01	465.70	0.007	323.152	0.86853	0.007	738.17	0.01
333.152	0.888832	0.01	468.77	0.009	333.152	0.862696	0.005	743.16	0.01
343.152	0.882998	0.006	471.87	0.006	343.152	0.856861	0.003	748.22	0.01
353.152	0.877206	0.004	474.99	0.001	353.152	0.851051	0.001	753.33	0.003
363.152	0.871446	0.01	478.12	0.012	363.152	0.845258	0.009	758.49	0.02
$[P_{4,4,4,4}][C_5COO]$					$[P_{4,4,4,4}][C_{11}COO]$				
293.150	0.922470	0.007	406.07	0.02	293.150	0.904566	0.008	507.15	0.02
298.152	0.919341	0.003	407.45	0.01	298.152	0.901469	0.004	508.89	0.01
303.152	0.916219	0.0005	408.84	0.0003	303.151	0.898381	0.0001	510.64	0.0007
313.152	0.909994	0.003	411.64	0.01	313.152	0.892221	0.005	514.17	0.01
323.152	0.903763	0.007	414.48	0.02	323.152	0.886089	0.007	517.72	0.02
333.152	0.897572	0.007	417.34	0.02	333.152	0.879979	0.007	521.32	0.02
343.152	0.891409	0.004	420.22	0.01	343.152	0.873891	0.004	524.95	0.01
353.152	0.885265	0.001	423.14	0.004	353.152	0.867825	0.001	528.62	0.004
363.152	0.879146	0.01	426.08	0.02	363.152	0.861787	0.01	532.32	0.02
$[P_{6,6,6,14}][C_{11}COO]$					$[P_{4,4,4,4}][c{-}C_6COO]$				
293.149	0.886997	0.0042	770.16	0.03	-	-	-	-	-
298.152	0.883890	0.0003	772.87	0.01	-	-	-	-	-
303.152	0.880793	0.003	775.59	0.004	-	-	-	-	-
313.152	0.874637	0.004	781.04	0.01	313.148	0.948335	0.006	407.66	0.008
323.152	0.868513	0.002	786.55	0.03	323.148	0.942133	0.002	410.35	0.001
333.152	0.862393	0.0002	792.13	0.03	333.148	0.935982	0.004	413.04	0.007
343.152	0.856288	0.004	797.78	0.02	343.148	0.929847	0.005	415.77	0.006
353.152	0.850154	0.005	803.54	0.0001	353.148	0.923757	0.001	418.51	0.002
363.152	0.843922	0.005	809.47	0.04	363.152	0.917701	0.007	421.27	0.008
$[P_{4,4,4,4}][PhC_1COO]$					$[P_{4,4,4,4}][TetrazC_1COO]$				

T / K	ρ / g cm^{-3}	δ / %	V_m / cm^3 mol^{-1}	δ / %	T / K	ρ / g cm^{-3}	δ / %	V_m / cm^3 mol^{-1}	δ / %
293.148	0.980931	0.01	402.25	0.01	293.15	1.031903	0.005	374.57	0.02
298.148	0.977809	0.006	403.53	0.005	-	-	-	-	
303.148	0.974695	0.0001	404.82	0.0005	303.152	1.025608	0.001	376.87	0.002
313.148	0.968507	0.008	407.41	0.007	313.152	1.019313	0.002	379.20	0.009
323.148	0.962358	0.01	410.01	0.01	323.152	1.013039	0.004	381.55	0.01
333.148	0.956251	0.01	412.63	0.009	333.152	1.006787	0.004	383.91	0.01
343.148	0.950195	0.006	415.26	0.006	343.152	1.000540	0.003	386.31	0.008
353.148	0.944169	0.002	417.91	0.002	353.152	0.994323	0.0004	388.73	0.003
363.152	0.938181	0.01	420.58	0.01	363.152	0.988133	0.006	391.16	0.01

Table S2 – Fitting parameters A_0 and A_1 determined from the linear fitting of the experimental densities to $\rho = A_0 + A_1 T$ and the corresponding absolute average deviation (AAD).

Sample	A_0 / g cm^{-3}	A_1 / g cm^{-3} K^{-1}	AAD / %
$[P_{4,4,4,4}][C_1COO]$	1.1158	-5.9409 x 10^{-4}	0.002
$[P_{4,4,4,4}][MeC_3COO]$	1.1043	-6.2047 x 10^{-4}	0.002
$[P_{4,4,4,4}][Me_4C_4COO]$	1.0852	-5.8903 x 10^{-4}	0.01
$[P_{6,6,6,14}][Me_4C_4COO]$	1.0578	-5.8538 x 10^{-4}	0.005
$[P_{4,4,4,4}][C_5COO]$	1.1039	-6.1924 x 10^{-4}	0.0005
$[P_{4,4,4,4}][C_{11}COO]$	1.0837	-6.1133 x 10^{-4}	0.005
$[P_{6,6,6,14}][C_{11}COO]$	1.0670	-6.1416 x 10^{-4}	0.003
$[P_{4,4,4,4}][c-C_6COO]$	1.1401	-6.1263 x 10^{-4}	0.004
$[P_{4,4,4,4}][PhC_1COO]$	1.1599	-6.1103 x 10^{-4}	0.008
$[P_{4,4,4,4}][TetrazC_1COO]$	1.2152	-6.2545 x 10^{-4}	0.003

Table S3 – Fitting parameters B_0 and B_1 determined from the linear fitting of the experimental molar volumes to $V_m = B_0 + B_1 T$ and the corresponding absolute average deviation (AAD).

Sample	M /g mol^{-1}	B_0/cm^3 mol^{-1}	B_1 /cm^3 mol^{-1} K^{-1}	AAD /%
$[P_{4,4,4,4}][C_1COO]$	318.48	272.20	0.22463	0.01
$[P_{4,4,4,4}][MeC_3COO]$	360.57	307.88	0.28166	0.005
$[P_{4,4,4,4}][Me_4C_4COO]$	416.66	366.15	0.30818	0.006
$[P_{6,6,6,14}][Me_4C_4COO]$	641.22	576.62	0.50029	0.01
$[P_{4,4,4,4}][C_5COO]$	374.59	322.26	0.28561	0.01
$[P_{4,4,4,4}][C_{11}COO]$	458.75	401.73	0.35920	0.01
$[P_{6,6,6,14}][C_{11}COO]$	683.13	605.92	0.59590	0.02
$[P_{4,4,4,4}][c-C_6COO]$	386.60	322.41	0.27214	0.005
$[P_{4,4,4,4}][PhC_1COO]$	394.58	325.50	0.26165	0.007
$[P_{4,4,4,4}][TetrazC_1COO]$	386.52	304.99	0.23707	0.01

Table S4 – Calculated densities of several ILs under study with the CL&Pol polarizable force field at different temperatures with the deviations from experiment densities.

Sample	$\frac{T}{\mathrm{K}}$	$\frac{\rho_{\mathrm{exp}}}{\mathrm{g\,cm^{-3}}}$	$\frac{\rho_{\mathrm{calc}}}{\mathrm{g\,cm^{-3}}}$	$\frac{\delta}{\%}$
$[P_{4,4,4,4}][C_1COO]$	343	0.911917	0.890728	-2.32
$[P_{4,4,4,4}][MeC_3COO]$	333	0.897580	0.876599	-2.33
	343	0.891380	0.866296	-2.81
	353	0.885180	0.863459	-2.45
$[P_{4,4,4,4}][Me_4C_4COO]$	303	0.906614	0.895556	-1.22
	343	0.882998	0.881350	-0.18
$[P_{6,6,6,14}][Me_4C_4COO]$	303	0.880298	0.889108	1.00
	343	0.856861	0.858520	0.19
$[P_{4,4,4,4}][C_5COO]$	303	0.916219	0.904468	-1.28
	323	0.903762	0.888582	-1.67
	343	0.891409	0.858099	-3.73
$[P_{4,4,4,4}][C_{11}COO]$	303	0.898381	0.897265	-0.12
	343	0.873891	0.857305	-1.89
$[P_{6,6,6,14}][C_{11}COO]$	303	0.880793	0.878202	-0.29
	343	0.856288	0.843112	-1.54
$[P_{4,4,4,4}][c{-}C_6COO]$	333	0.935982	0.901587	-3.67
	343	0.929847	0.897665	-3.46
$[P_{4,4,4,4}][PhC_1COO]$	303	0.974695	0.976053	0.14
	323	0.962358	0.960491	-0.19
	343	0.950195	0.937350	-1.35
$[P_{4,4,4,4}][p{-}MeBzCOO]$	363	-	0.936795	-
	373	-	0.903211	-
$[P_{4,4,4,4}][TetrazC_1COO]$	303	1.025608	1.035093	0.92
	343	1.000540	1.031101	3.05

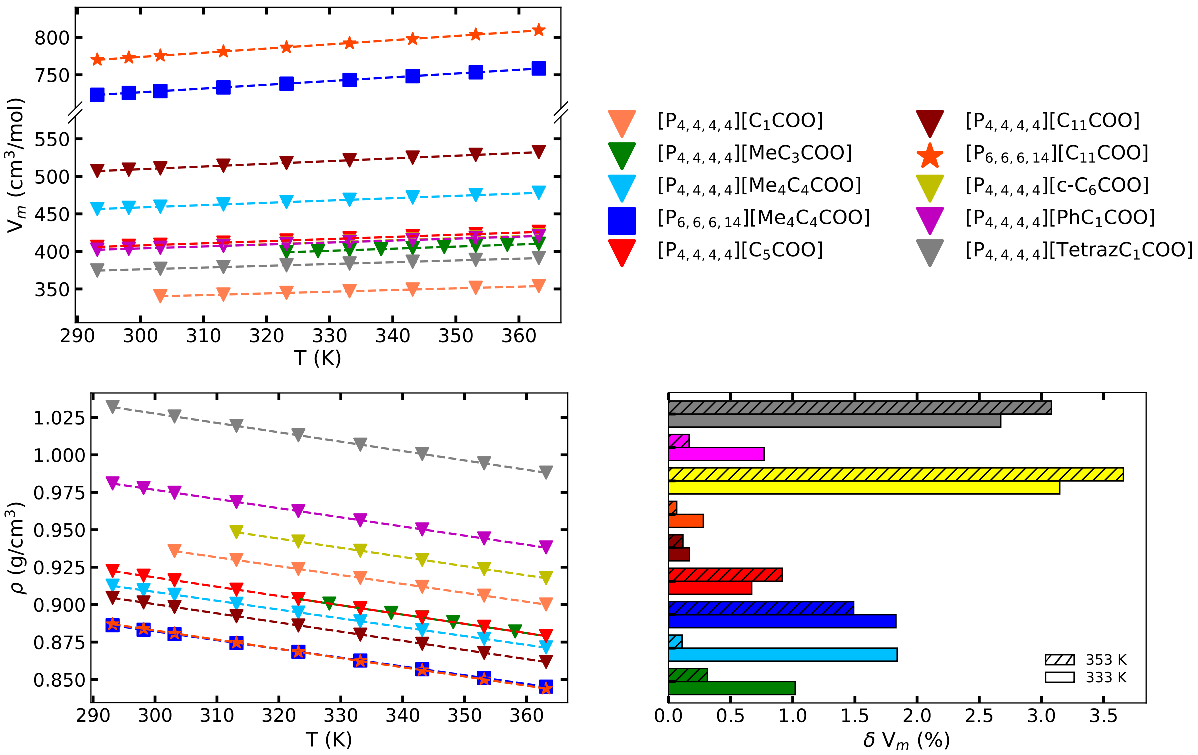

Figure S2 – Experimental molar volumes (top-left) and densities (bottom-left) of the pure ILs as a function of temperature, with linear fits (dashed lines). (Bottom-right) Deviation of the predicted molar volumes (V_m pred.) determined by the GCM from the experimental values (V_m exp.) at 333.15 and 353.15 K.

Table S5 – Group contribution parameters used to calculate the molar volume of cation and anion as a function of temperature.

Group j	C_0	C_1	C_2	Ref
	cm^3 mol^{-1}	cm^3 mol^{-1} K	cm^3 mol^{-1} K^2	
$-CH_2$	16.967	1.399 x 10^{-3}	-1.946 x 10^{-6}	2
$-CH_3$ (branched compound)	14.460	-3.593 x 10^{-2}	8.574 x 10^{-4}	2⋆
$-C_6H_{11}$	99.909	3.164 x 10^{-2}	5.004 x 10^{-4}	3† 4⋆
$-CH_2-Ph$	80.185	1.344 x 10^{-1}	1.230 x 10^{-4}	2⋆
$-COO^-$	21.680	3.101 x 10^{-2}	-4.333 x 10^{-4}	5
$-CH_3COO^-$	49.177	2.149 x 10^{-2}	-2.775 x 10^{-5}	2
$-$Tetraz	52.187	-1.791 x 10^{-2}	-5.598 x 10^{-5}	6†
$[P_{4,4,4,4}]^+$	290.987	3.192 x 10^{-1}	1.436 x 10^{-5}	2⋆
$[P_{6,6,6,14}]^+$	560.514	3.904 x 10^{-1}	1.184 x 10^{-4}	2

⋆ Calculated by subtraction of parameters available in the reference.

† Calculated from the density data from the reference with temperatures ranging from 293.15 to 323.15 K for $-C_6H_{11}$ and 283.15 to 353.15 K for $-$Tetraz.

Table S6 – Number of groups (n_j) considered for the calculation of the molar volume of the studied ILs using the group contribution method (GCM) as well as the experimental molar volumes (V_m exp.) and the predicted ones (V_m pred.) at temperatures ranging from 293.15 to 363.15 K depending on the melting point of the IL.

Group j	n_j	$\frac{T}{K}$	$\frac{V_m \text{ exp.}}{\text{cm}^3\text{ mol}^{-1}}$	$\frac{V_m \text{ pred.}}{\text{cm}^3\text{ mol}^{-1}}$	$\frac{\delta}{\%}$
$[P_{4,4,4,4}][MeC_3COO]$					
$-CH_2$	1	323.15	398.93	393.86	1.27
$-CH_3$ (branched)	2	333.15	401.71	397.59	1.02
$-CH_3COO^-$	1	353.15	407.34	406.06	0.31
$[P_{4,4,4,4}]^+$	1	363.15	410.20	410.80	0.14
$[P_{4,4,4,4}][Me_4C_4COO]$					
$-CH_2$	2	293.15	458.05	445.61	2.39
$-CH_3$ (branched)	5	313.15	462.64	450.51	2.62
$-CH_3COO^-$	1	333.15	468.77	460.12	1.84
$[P_{4,4,4,4}]^+$	1	353.15	474.99	474.43	0.12
$[P_{6,6,6,14}][Me_4C_4COO]$					
$-CH_2$	2	293.15	723.42	714.85	1.18
$-CH_3$ (branched)	5	313.15	733.22	720.44	1.74
$-CH_3COO^-$	1	333.15	743.16	729.51	1.84
$[P_{6,6,6,14}]^+$	1	353.15	753.33	742.08	1.49
$[P_{4,4,4,4}][C_5COO]$					
$-CH_2$	4	293.15	406.07	406.30	0.06
$-CH_3COO^-$	1	333.15	417.34	420.13	0.67
$[P_{4,4,4,4}]^+$	1	353.15	423.14	427.01	0.91
$[P_{4,4,4,4}][C_{11}COO]$					
$-CH_2$	10	293.15	507.15	508.06	0.18
$-CH_3COO^-$	1	333.15	521.32	522.21	0.17
$[P_{4,4,4,4}]^+$	1	353.15	528.62	529.24	0.11
$[P_{6,6,6,14}][C_{11}COO]$					
$-CH_2$	10	293.15	770.16	777.23	0.91
$-CH_3COO^-$	1	333.15	792.13	794.35	0.28
$[P_{6,6,6,14}]^+$	1	353.15	803.54	803.00	0.06
$[P_{4,4,4,4}][c-C_6COO]$					
$-C_6H_{11}$	1	313.15	407.66	418.32	2.61
$-COO^-$	1	333.15	413.04	426.04	3.15
$[P_{4,4,4,4}]^+$	1	353.15	418.51	433.82	3.66
$[P_{4,4,4,4}][PhC_1COO]$					
$-CH_2-Ph$	1	293.15	402.25	390.42	2.94
$-COO^-$	1	333.15	412.63	409.45	0.77
$[P_{4,4,4,4}]^+$	1	353.15	417.91	418.61	0.16
$[P_{4,4,4,4}][TetrazC_1COO]$					
$-CH_2$	1	293.15	374.57	379.96	1.43
$-COO^-$	1	313.15	379.20	387.26	2.12
$-$Tetraz	1	333.15	383.91	394.17	2.67
$[P_{4,4,4,4}]^+$	1	353.15	388.73	400.70	3.08

Table S7 – Experimental viscosities of the ILs in the temperature range of 293–363 K. The deviations (δ) reported are relative to the fitting of the VFT function with coefficients listed in Table S8.

T / K	η / mPa s	δ / %	T / K	η / mPa s	δ / %	T / K	η / mPa s	δ / %
$[P_{4,4,4,4}][C_1COO]$			$[P_{4,4,4,4}][MeC_3COO]$			$[P_{4,4,4,4}][Me_4C_4COO]$		
-	-	-	-	-	-	298.15	1344	0.01
-	-	-	-	-	-	303.15	900.6	0.02
-	-	-	-	-	-	313.15	439.5	0.06
-	-	-	-	-	-	323.15	236.3	0.3
333.16	67.10	0.04	333.15	52.94	0.1	333.15	136.2	0.02
343.15	43.13	0.04	343.15	34.39	0.1	343.15	83.50	0.4
353.15	29.10	0.03	353.15	23.42	0.2	353.15	54.17	0.4
-	-	-	363.15	16.79	0.2	363.15	36.76	0.3
$[P_{6,6,6,14}][Me_4C_4COO]$			$[P_{4,4,4,4}][C_5COO]$			$[P_{4,4,4,4}][C_{11}COO]$		
293.15	1253	0.05	293.15	548.9	0.03	293.15	574.4	0.02
298.15	889.4	0.08	298.15	377.3	0.12	298.15	403.6	0.06
303.15	644.9	0.1	303.15	266.8	0.06	303.15	290.6	0.06
313.15	356.5	0.7	313.15	142.9	0.91	313.15	160.1	0.4
323.15	221.0	3.8	323.15	86.05	1.30	323.15	96.01	0.3
333.15	130.7	1.4	333.15	53.45	0.23	333.15	60.54	0.09
343.15	84.69	2.3	-	-	-	343.15	40.32	0.06
353.15	57.19	2.8	-	-	-	353.15	28.14	0.4
363.15	40.06	3.2	-	-	-	363.15	20.36	0.8
$[P_{6,6,6,14}][C_{11}COO]$			$[P_{4,4,4,4}][c-C_6COO]$			$[P_{4,4,4,4}][PhC_1COO]$		
293.15	598.4	0.05	-	-	-	293.15	529.2	0.03
298.15	434.2	0.07	-	-	-	298.15	365.8	0.1
303.15	321.3	0.1	-	-	-	303.15	259.3	0.07
313.15	185.9	0.5	313.15	505.7	0.01	313.15	140.9	0.1
323.15	110.9	2.2	323.15	254.3	0.1	323.15	83.05	0.2
333.15	72.34	1.0	333.15	140.2	0.1	333.15	52.39	0.3
343.15	49.56	0.7	343.15	83.55	0.3	343.15	35.15	0.2
353.15	35.35	2.7	353.15	53.12	0.2	353.15	24.73	1.0
363.15	26.09	4.8	363.15	36.13	1.3	363.15	18.09	1.9
$[P_{4,4,4,4}][TetrazC_1COO]$								
303.15	1425	0.003						
313.15	595.0	0.07						
323.15	285.1	0.4						
333.15	149.9	0.4						
343.15	86.10	0.6						
353.15	53.31	0.2						
363.15	35.28	1.3						

Table S8 – Fitting parameters A, B and T_0 determined from the fitting of the experimental viscosities to the VFT function and the corresponding absolute average deviation (AAD).

Sample	A (mPa s)	B (K)	T_0 (K)	AAD (%)
$[P_{4,4,4,4}][C_1COO]$	0.0326	1241.10	170.50	0.04
$[P_{4,4,4,4}][MeC_3COO]$	0.0713	940.49	190.91	0.13
$[P_{4,4,4,4}][Me_4C_4COO]$	0.0288	1390.59	168.80	0.19
$[P_{6,6,6,14}][Me_4C_4COO]$	0.0194	1741.66	135.87	1.6
$[P_{4,4,4,4}][C_5COO]$	0.0695	1025.62	178.88	0.04
$[P_{4,4,4,4}][C_{11}COO]$	0.0388	1256.02	162.36	0.20
$[P_{6,6,6,14}][C_{11}COO]$	0.0256	1522.16	141.84	1.3
$[P_{4,4,4,4}][c-C_6COO]$	0.0492	1147.23	188.97	0.40
$[P_{4,4,4,4}][PhC_1COO]$	0.0591	1070.43	175.52	0.47
$[P_{4,4,4,4}][TetrazC_1COO]$	0.0347	1187.17	191.40	0.40

Thermal stability analysis

Table S9 – Glass transition temperatures (T_g), melting points (T_{fus}) and crystallization temperatures (T_{cr}) for the pure ILs and the mixtures prepared. The different temperatures reported were measured using DSC with a 10 K min^{-1} heating rate. In order to facilitate the reading, when the onset temperature is reported, the value will be followed by (o) and when the peak temperature is reported, a (p) marker is used.

Sample	T_g (°C)	T_{trans} (°C) & T_{fus} (°C)	T_{cr} (°C)
$[P_{4,4,4,4}][C_1COO]$	-	22.6 (o) & 49.3 (o)	13.1 (o)
$[P_{4,4,4,4}][MeC_3COO]$	-52.8	-8.0 (p) & 66.0 (p)	-16.6 (p)
$[P_{4,4,4,4}][Me_4C_4COO]$	-56.3	0.7 (p) & 34.2 (p)	-18.3 (p)
$[P_{6,6,6,14}][Me_4C_4COO]$	-65.8	-	-
$[P_{4,4,4,4}][C_5COO]$	-65.1	-	-
$[P_{4,4,4,4}][C_{11}COO]$	-65.3	-	-
$[P_{6,6,6,14}][C_{11}COO]$	-	-20.8 (o) & -17.1 (o)	-26.9 (o)
$[P_{4,4,4,4}][c-C_6COO]$	-44.6	61.8 (p)	46.3 (p)
$[P_{4,4,4,4}][PhC_1COO]$	-63.9	-8.5 (p) & 44.1 (o)	7.2 (o)
$[P_{4,4,4,4}][p-MeBzCOO]$	-	90.7 (o)	11.6 (o)
$[P_{4,4,4,4}][TetrazC_1COO]$	-	9.1 (o)	-37.4 (p)

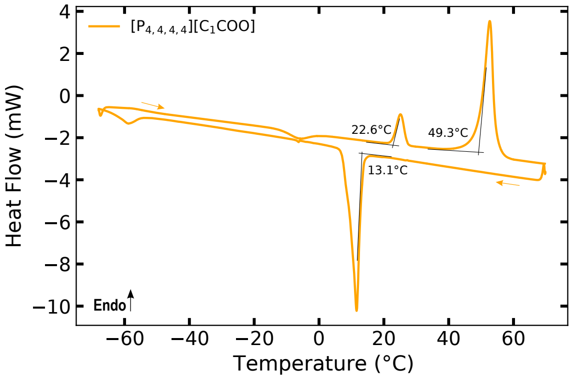
[P$_{4,4,4,4}$][C$_1$COO]
22.6°C
49.3°C
13.1°C
Endo
Heat Flow (mW)
4
2
0
−2
−4
−6
−8
−10
−60
−40
−20
0
20
40
60
Temperature (°C)

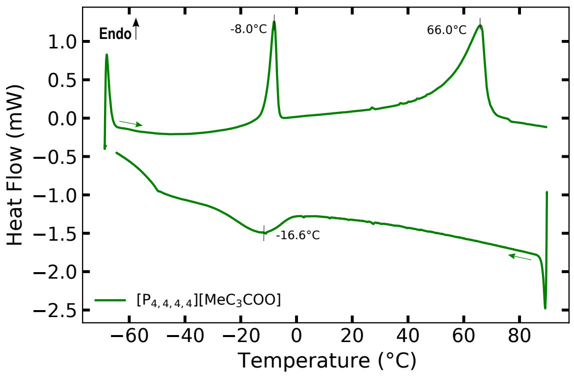
Endo
-8.0°C
66.0°C
-16.6°C
[P$_{4,4,4,4}$][MeC$_3$COO]
Heat Flow (mW)
1.0
0.5
0.0
−0.5
−1.0
−1.5
−2.0
−2.5
−60
−40
−20
0
20
40
60
80
Temperature (°C)

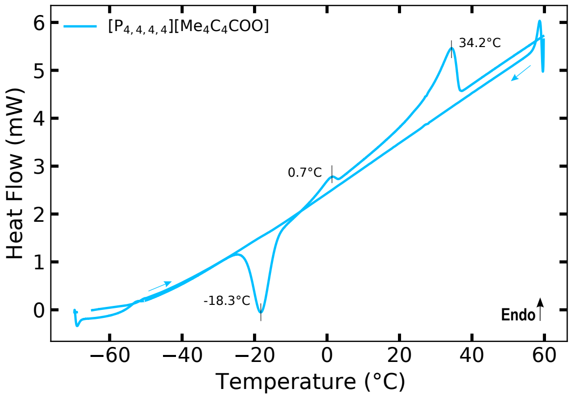
[P$_{4,4,4,4}$][Me$_4$C$_4$COO]
34.2°C
0.7°C
-18.3°C
Endo
Heat Flow (mW)
6
5
4
3
2
1
0
−60
−40
−20
0
20
40
60
Temperature (°C)

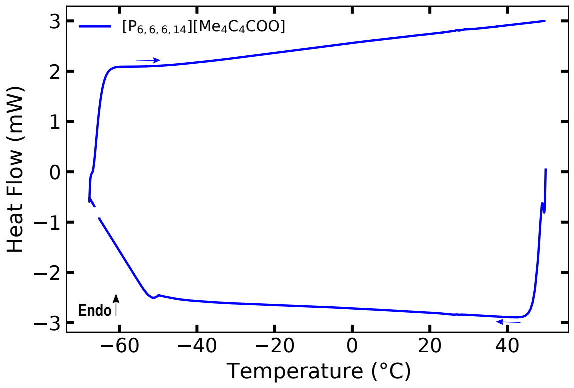
[P$_{6,6,6,14}$][Me$_4$C$_4$COO]
Endo
Heat Flow (mW)
3
2
1
0
−1
−2
−3
−60
−40
−20
0
20
40
Temperature (°C)

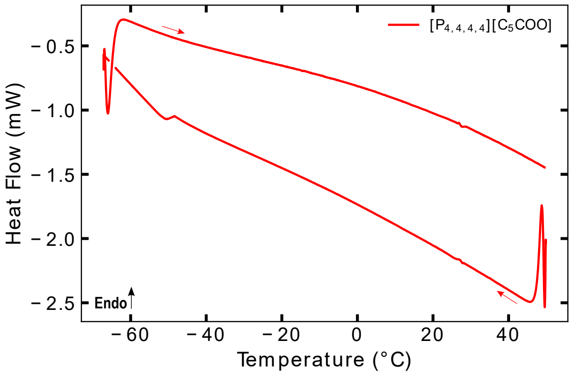
[P$_{4,4,4,4}$][C$_5$COO]
Endo
Heat Flow (mW)
− 0.5
− 1.0
− 1.5
− 2.0
− 2.5
− 60
− 40
− 20
0
20
40
Temperature (°C)

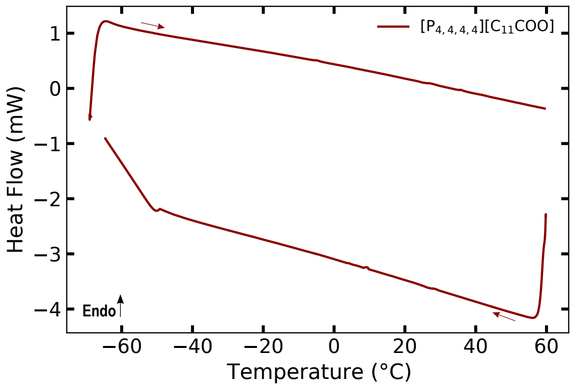
[P$_{4,4,4,4}$][C$_{11}$COO]
Endo
Heat Flow (mW)
1
0
−1
−2
−3
−4
−60
−40
−20
0
20
40
60
Temperature (°C)

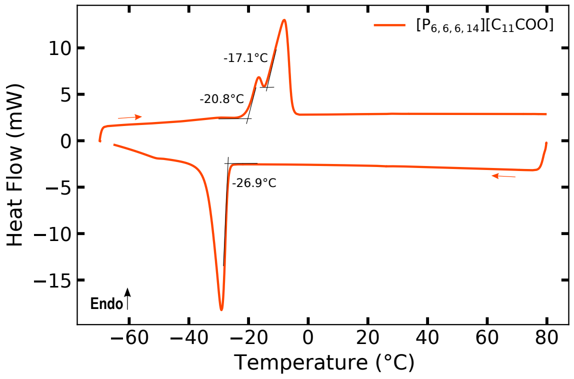
[P$_{6,6,6,14}$][C$_{11}$COO]
-17.1°C
-20.8°C
-26.9°C
Endo
Heat Flow (mW)
10
5
0
−5
−10
−15
−60
−40
−20
0
20
40
60
80
Temperature (°C)

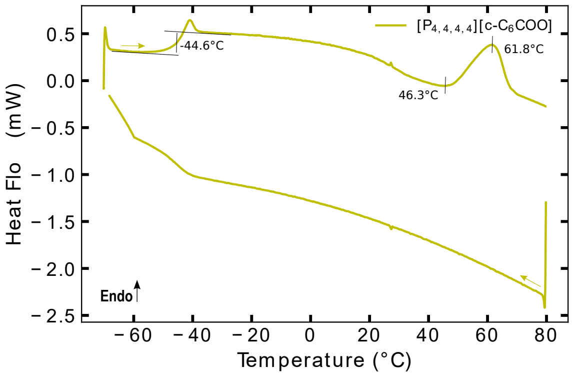
[P$_{4,4,4,4}$][c-C$_6$COO]
-44.6°C
61.8°C
46.3°C
Endo
Heat Flo (mW)
0.5
0.0
− 0.5
− 1.0
− 1.5
− 2.0
− 2.5
− 60
− 40
− 20
0
20
40
60
80
Temperature (°C)

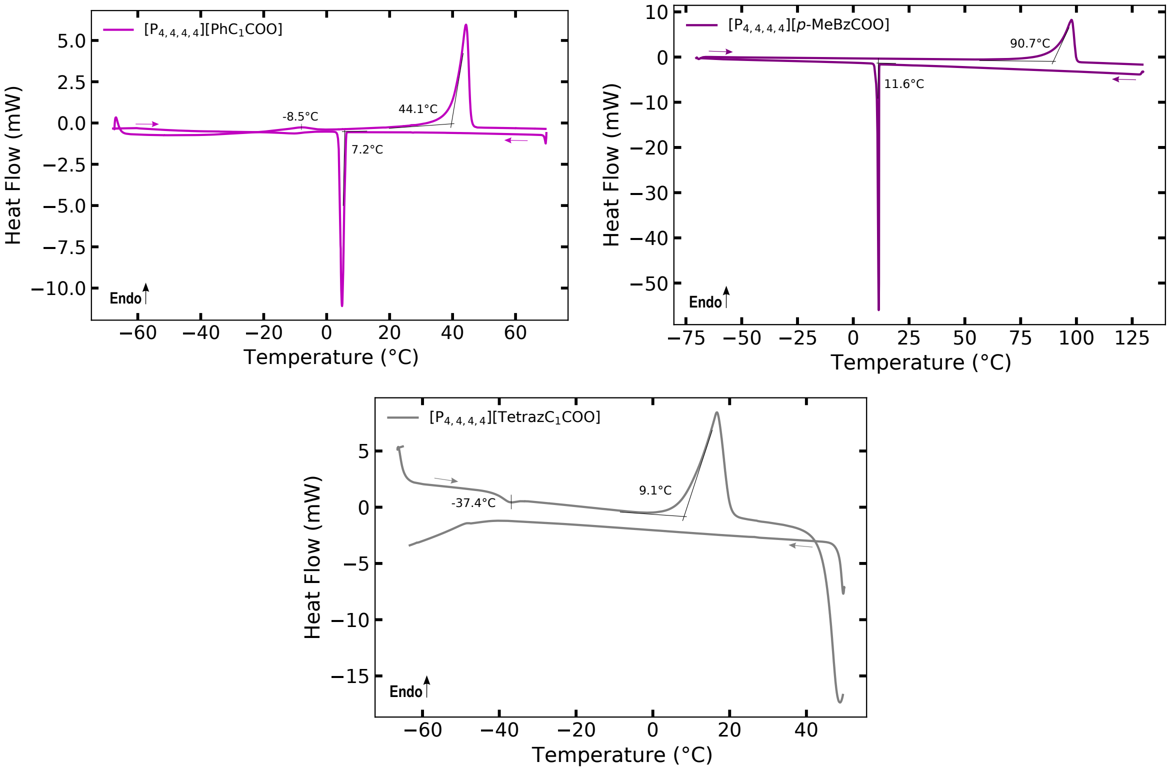

Figure S3 – DSC traces of 🟧 $[P_{4,4,4,4}][C_1COO]$, 🟥 $[P_{4,4,4,4}][C_5COO]$, 🟫 $[P_{4,4,4,4}][C_{11}COO]$, 🟧 $[P_{6,6,6,14}][C_{11}COO]$, 🟩 $[P_{4,4,4,4}][MeC_3COO]$, 🟦 $[P_{4,4,4,4}][Me_4C_4COO]$, 🟦 $[P_{6,6,6,14}][Me_4C_4COO]$, 🟨 $[P_{4,4,4,4}][c{-}C_6COO]$, 🟪 $[P_{4,4,4,4}][PhC_1COO]$, 🟪 $[P_{4,4,4,4}][p{-}MeBzCOO]$ and ⬜ $[P_{4,4,4,4}][TetrazC_1COO]$ measured at 10 K min^{-1}.

Table S10 – Decomposition temperatures (T_{dec}) for the pure ILs and a few ILs mixtures determined at 10 °C min^{-1} under an atmosphere of N_2 or O_2.

Sample	Atm	$T_{dec,1}$ (°C)	$T_{dec,2}$ (°C)
$[P_{4,4,4,4}][C_1COO]$	N_2[7]	317	-
	O_2	325	-
$[P_{4,4,4,4}][MeC_3COO]$	N_2	292	-
	O_2	328	-
$[P_{4,4,4,4}][Me_4C_4COO]$	O_2	319	-
$[P_{6,6,6,14}][Me_4C_4COO]$	O_2	342	-
$[P_{4,4,4,4}][C_5COO]$	N_2	302	-
	O_2	328	-
$[P_{4,4,4,4}][C_{11}COO]$	N_2	274	-
	O_2	344	-
$[P_{6,6,6,14}][C_{11}COO]$	N_2	318	-
	O_2	345	-
$[P_{4,4,4,4}][c-C_6COO]$	N_2	303	-
	O_2	336	-
$[P_{4,4,4,4}][PhC_1COO]$	N_2	256	358
	O_2	254	-
$[P_{4,4,4,4}][p-MeBzCOO]$	N_2	337	-
	O_2	363	-
$[P_{4,4,4,4}][TetrazC_1COO]$	O_2	291	-

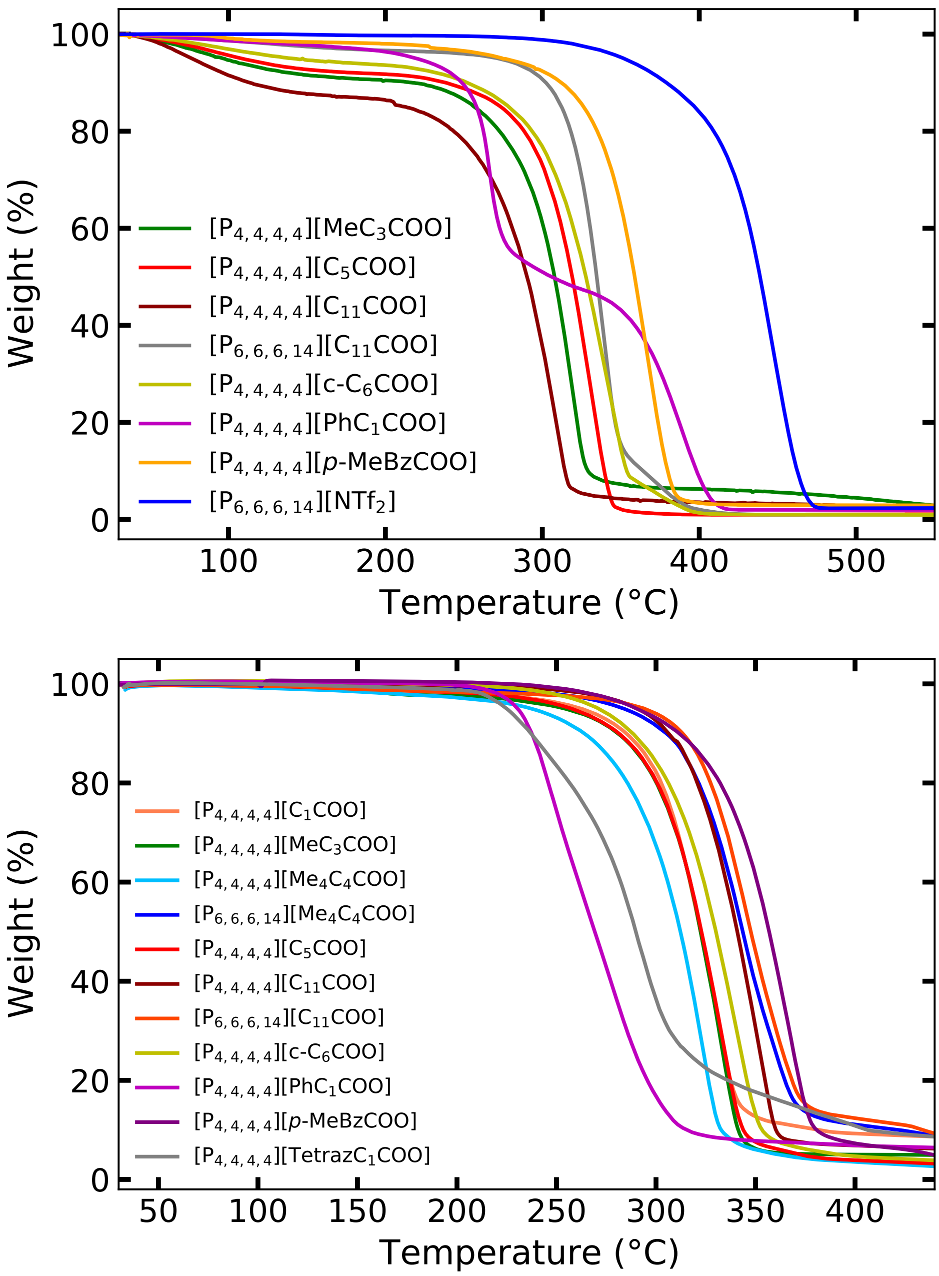

Figure S4 – TGA thermographs of the ILs with a heat rate of 10 °C min^{-1} under: N_2 (top) and O_2 (bottom). The decomposition temperatures were determined by the intersection of the tangents to the lines at low temperature and those corresponding to the rapid mass loss.

Molecular Dynamics Simulations

Table S11 – Simulated self-diffusion coefficients of various ILs at different temperatures by fitting the MSD calculated from MD simulations.

Sample (simulated)	T (K)	D_{anion} (10^{-11} m^2 s^{-1})	D_{cation} (10^{-11} m^2 s^{-1})
$[P_{4,4,4,4}][C_1COO]$	343	1.60 ± 0.02	1.46 ± 0.02
$[P_{4,4,4,4}][MeC_3COO]$	343	2.44 ± 0.01	2.35 ± 0.01
$[P_{4,4,4,4}][Me_4C_4COO]$	343	1.91 ± 0.02	1.75 ± 0.03
$[P_{6,6,6,14}][Me_4C_4COO]$	343	0.98 ± 0.07	1.02 ± 0.04
$[P_{4,4,4,4}][C_5COO]$	303	1.01 ± 0.06	0.99 ± 0.06
	343	4.79 ± 0.02	4.32 ± 0.02
$[P_{4,4,4,4}][C_{11}COO]$	303	1.26 ± 0.04	0.91 ± 0.04
	343	3.50 ± 0.08	3.18 ± 0.09
$[P_{6,6,6,14}][C_{11}COO]$	303	0.67 ± 0.02	0.52 ± 0.01
	343	1.55 ± 0.03	1.58 ± 0.03
$[P_{4,4,4,4}][c{-}C_6COO]$	333	1.19 ± 0.04	1.00 ± 0.03
	343	1.34 ± 0.03	1.27 ± 0.03
$[P_{4,4,4,4}][PhC_1COO]$	343	4.06 ± 0.02	3.97 ± 0.02
$[P_{4,4,4,4}][p{-}MeBzCOO]$	373	4.99 ± 0.02	4.16 ± 0.02
$[P_{4,4,4,4}][TetrazC_1COO]$	343	1.40 ± 0.03	2.66 ± 0.01

Table S12 – Distance between the centres of mass between of the fragments used calculated by DFT at the B97-D3/cc-pVDZ level.

Dimers	r (Å)
$[P_{1,1,1,1}]^+$-$[C_1COO]^-$	3.855
$[P_{1,1,1,1}]^+$-Toluene	4.467
$[P_{1,1,1,1}]^+$-Cyclohexane	5.667
$[P_{1,1,1,1}]^+$-Tetrazole	5.789
Toluene-$[C_1COO]^-$ ($[p{-}MeBzCOO]^-$)	5.561
Toluene-$[C_1COO]^-$ ($[PhC_1COO]^-$)	5.221
Toluene-Toluene	6.383
Cyclohexane-$[C_1COO]^-$	5.311
Cyclohexane-Butane	5.125
Cyclohexane-Cyclohexane	6.062
Tetrazole-$[C_1COO]^-$	4.221
Tetrazole- Butane	5.904
Tetrazole-Tetrazole	4.997

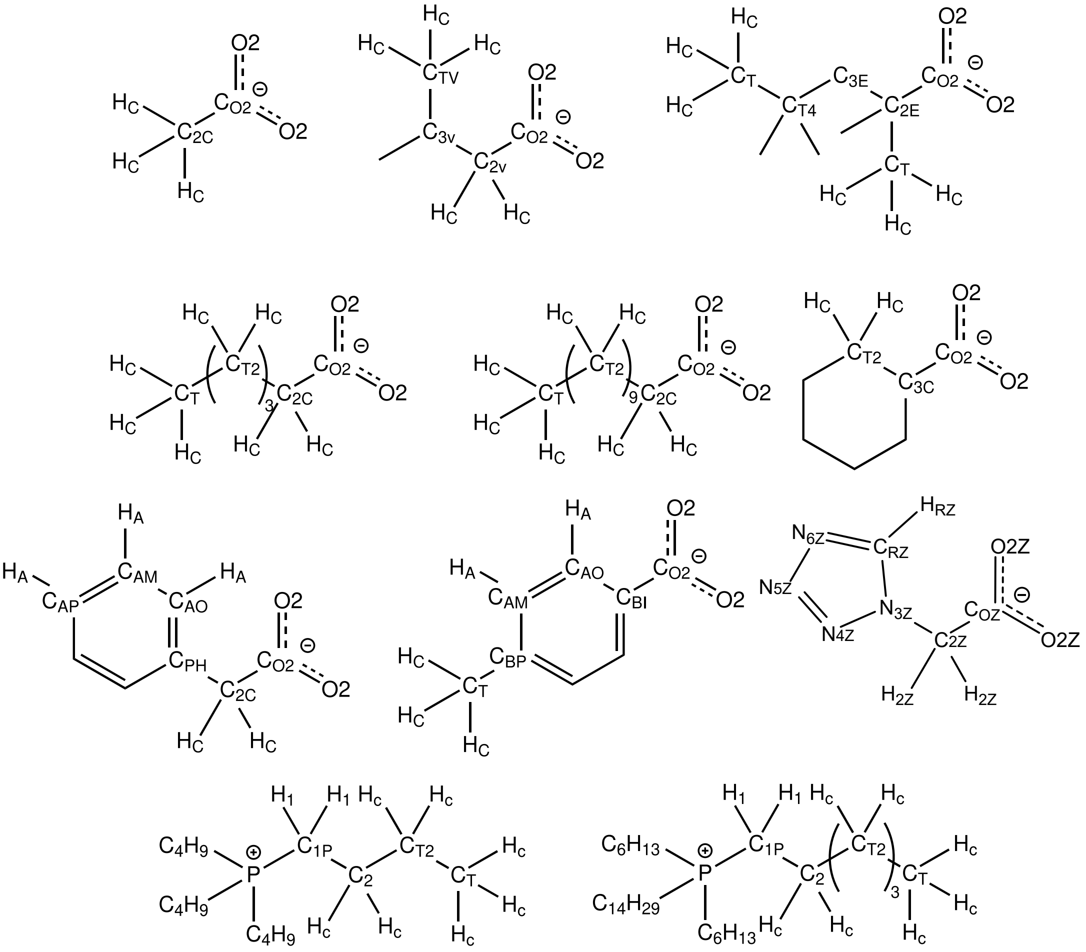

Figure S5 – Atom site labels and structure of the simulated ILs. The unlabelled atoms are the same as the respectively labelled symmetric sites.

Table S13 – New dihedral parameters used for [TetrazC$_1$COO]$^-$. Other atoms use the parameters from OPLS-AA and CL&Pol force fields with the corresponding atom type labels.

Ion	Dihedral	v1	v2	v3	v4
[TetrazC$_1$COO]$^-$	NNCC	-37.0894	5.1348	-1.8911	0.9450
	NCCO	0.10955	-1.2516	-0.101	1.09295

Table S14 – New force field parameters used for $[\mathrm{MeC_3COO}]^-$, $[\mathrm{c{-}C_6COO}]^-$, $[\mathrm{PhC_1COO}]^-$, $[p{-}\mathrm{MeBzCOO}]^-$ and $[\mathrm{TetrazC_1COO}]^-$. Other atoms use the parameters from OPLS-AA and CL&Pol force fields with the corresponding atom type labels.

Ion	Atom type	q (e)	σ (Å)	ϵ (kJ mol^{-1})
$[\mathrm{MeC_3COO}]^-$	$\mathrm{C_{2V}}$	-0.300	3.50	0.27614
	$\mathrm{C_{3V}}$	0.420	3.50	0.27614
	$\mathrm{C_{TV}}$	-0.380	3.50	0.27614
$[\mathrm{Me_4C_4COO}]^-$	$\mathrm{C_{2E}}$	0.280	3.50	0.27614
	$\mathrm{C_{3E}}$	-0.500	3.50	0.27614
	$\mathrm{C_{T4}}$	0.000	3.50	0.27614
$[\mathrm{c{-}C_6COO}]^-$	$\mathrm{C_{3C}}$	-0.160	3.50	0.27614
$[\mathrm{PhC_1COO}]^-$	$\mathrm{C_{PH}}$	0.163	3.55	0.29288
$[p{-}\mathrm{MeBzCOO}]^-$	$\mathrm{C_{BI}}$	-0.040	3.55	0.29288
	$\mathrm{C_{BP}}$	0.064	3.55	0.29288
$[\mathrm{TetrazC_1COO}]^-$	$\mathrm{O_{2Z}}$	-0.730	2.96	0.87864
	$\mathrm{C_{OZ}}$	0.840	3.75	0.43932
	$\mathrm{C_{2Z}}$	-0.740	3.50	0.27614
	$\mathrm{H_{2Z}}$	0.180	2.50	0.12552
	$\mathrm{C_{RZ}}$	0.140	3.55	0.29288
	$\mathrm{H_{RZ}}$	0.115	2.42	0.12552
	$\mathrm{N_{3Z}}$	0.685	3.25	0.71128
	$\mathrm{N_{4Z}}$	-0.420	3.25	0.71128
	$\mathrm{N_{5Z}}$	-0.100	3.25	0.71128
	$\mathrm{N_{6Z}}$	-0.420	3.25	0.71128

Table S15 – The scaling factors evaluated for the dispersion energy (ϵ) of the LJ potential.

Dimers	k
$[\mathrm{P_{1,1,1,1}}]^+$-$[\mathrm{C_1COO}]^-$	0.44
$[\mathrm{P_{1,1,1,1}}]^+$-Butane	0.65
$[\mathrm{P_{1,1,1,1}}]^+$-Toluene	0.64
$[\mathrm{P_{1,1,1,1}}]^+$-Cyclohexane	0.53
$[\mathrm{P_{1,1,1,1}}]^+$-Tetrazole	0.52
Toluene-$[\mathrm{C_1COO}]^-$	0.42
Butane-$[\mathrm{C_1COO}]^-$	0.50
Cyclohexane-$[\mathrm{C_1COO}]^-$	0.41
Tetrazole-$[\mathrm{C_1COO}]^-$	0.50
Toluene-Butane	0.90
Toluene-Toluene	1.00
Cyclohexane-Butane	1.00
Butane-Butane	0.94
Cyclohexane-Cyclohexane	1.00
Tetrazole-Butane	1.00
Tetrazole-Tetrazole	1.00

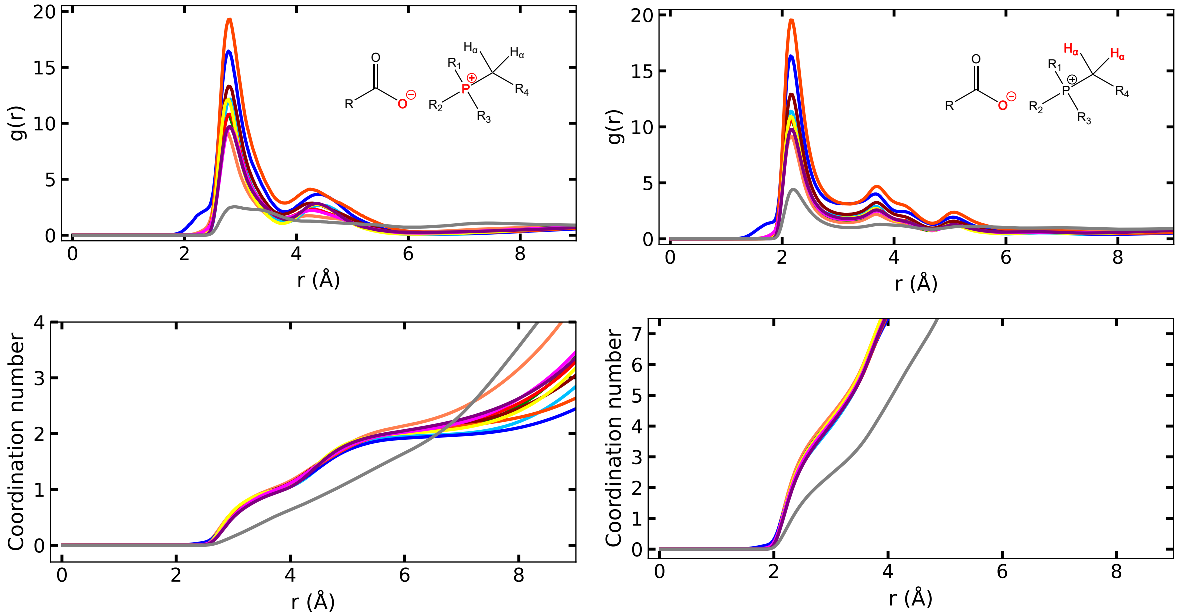

Figure S6 – Comparison of the site-site RDFs, g(r), of (left) the P^+ and (right) the H_α of the cation around the negatively charged oxygen atoms O^-_{COO} of the carboxylate head of the anion and their corresponding coordination numbers in 🟧 $[P_{4,4,4,4}][C_1COO]$, 🟩 $[P_{4,4,4,4}][MeC_3COO]$, 🟦 $[P_{4,4,4,4}][Me_4C_4COO]$, 🟦 $[P_{6,6,6,14}][Me_4C_4COO]$, 🟥 $[P_{4,4,4,4}][C_5COO]$, 🟫 $[P_{4,4,4,4}][C_{11}COO]$, 🟧 $[P_{6,6,6,14}][C_{11}COO]$, 🟨 $[P_{4,4,4,4}][c-C_6COO]$, 🟪 $[P_{4,4,4,4}][PhC_1COO]$ and ⬜ $[P_{4,4,4,4}][TetrazC_1COO]$ at 343 K and at 373 K for 🟪 $[P_{4,4,4,4}][p-MeBzCOO]$.

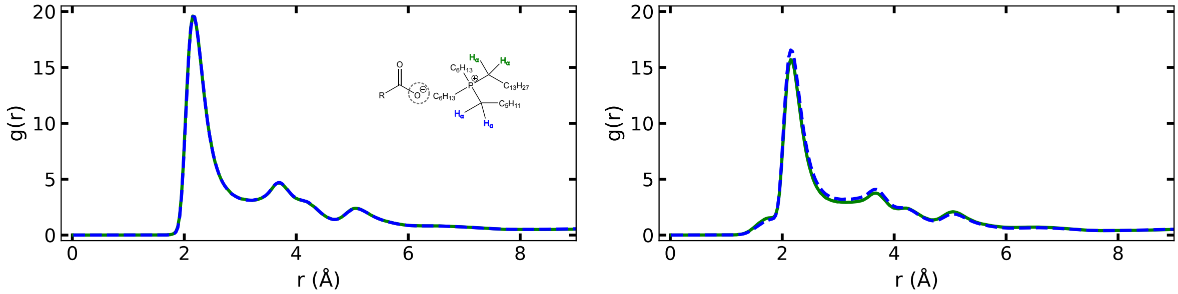

Figure S7 – Site-site RDF, g(r), of the H_α of the 🟩 tetradecyl (C_{14}) and of the 🟦 hexyl (C_6) alkyl side chains of the cation around the carboxylate head of the anion in (left) $[P_{6,6,6,14}][C_{11}COO]$ and (right) $[P_{6,6,6,14}][Me_4C_4COO]$ at 343 K.

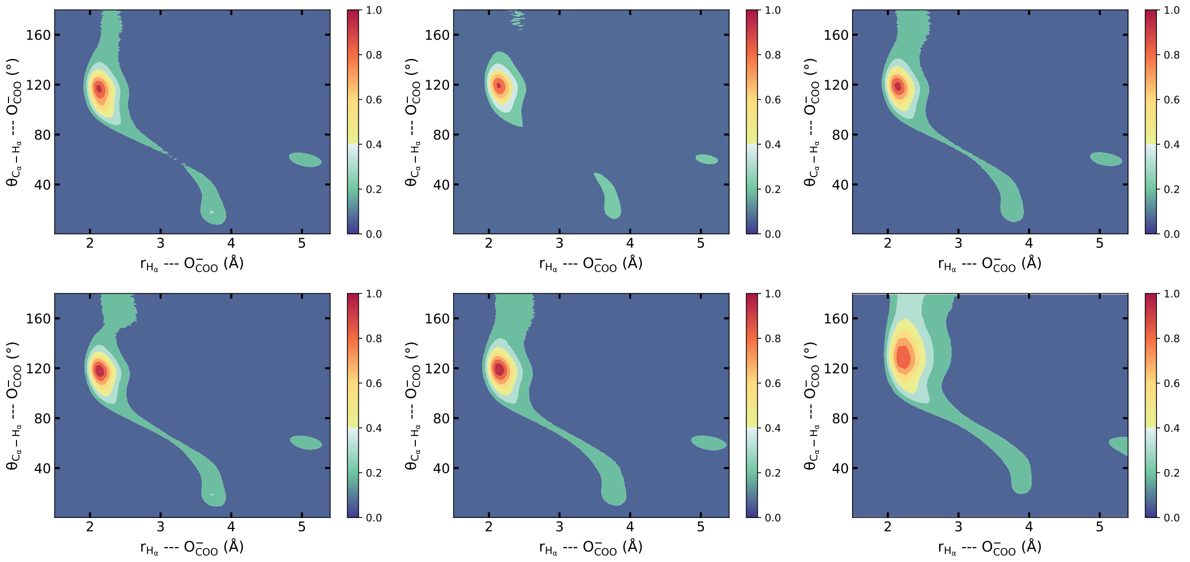

Figure S8 – Combined distribution function (CDF) of the $C_\alpha{-}H_\alpha\cdots O^-_{COO}$ angle as a function of the distance between the acidic proton H_α and the negatively charged O^-_{COO} in (top left) $[P_{4,4,4,4}][C_1COO]$, (top middle) $[P_{4,4,4,4}][Me_4C_4COO]$, (top right) $[P_{4,4,4,4}][C_{11}COO]$, (bottom left) $[P_{4,4,4,4}][c{-}C_6COO]$, (bottom middle) $[P_{4,4,4,4}][PhC_1COO]$ and (bottom right) $[P_{4,4,4,4}][TetrazC_1COO]$ at 343 K.

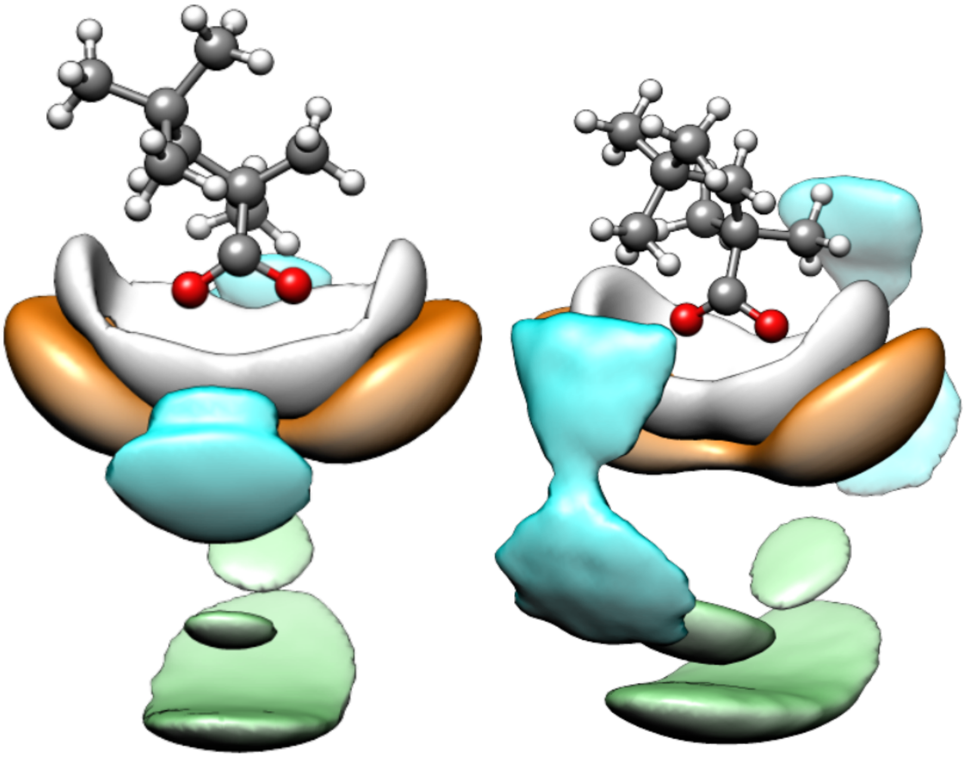

Figure S9 – SDFs of P^+ (in orange), of H_α (in white), of the terminal carbon atoms of the alkyl chains of the cation (in blue) and of the terminal carbon of the branched alkyl chain belonging to $[Me_4C_4COO]^-$ (in green) with (left) $[P_{4,4,4,4}]^+$ cation and (right) $[P_{6,6,6,14}]^+$ cation around O^-_{COO} of the anion at 343 K.

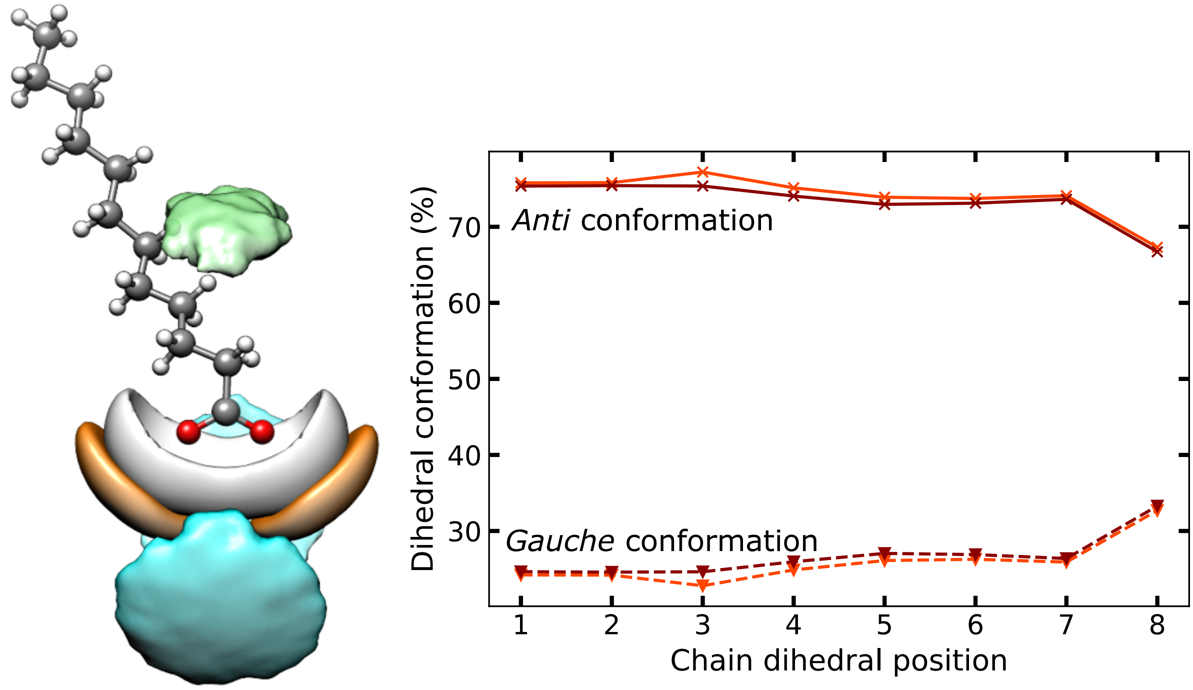

Figure S10 – (Left) SDFs of P$^+$ (in orange), of H$_\alpha$ (in white), of the terminal carbon atoms of the alkyl chains of [P$_{6,6,6,14}$]$^+$ (in blue) and of the terminal carbon of [C$_{11}$COO]$^-$ (in green) around O$^-_{COO}$ of the anion in [P$_{6,6,6,14}$][C$_{11}$COO] at 343 K. (Right) Average *gauche* and *anti* conformation percentage for each C−C−C−C dihedral angle along the dodecyl chain of the [C$_{11}$COO]$^-$ anion in [P$_{4,4,4,4}$][C$_{11}$COO] and [P$_{6,6,6,14}$][C$_{11}$COO].

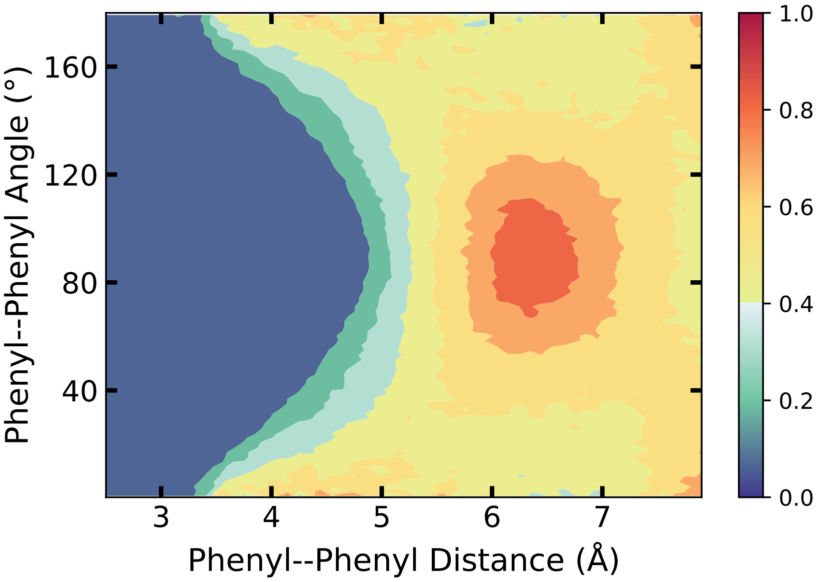

Figure S11 – CDF of the angle between two adjacent phenyl rings as a function of the RDF between their center of mass in [P$_{4,4,4,4}$][p−MeBzCOO] at 343 K.

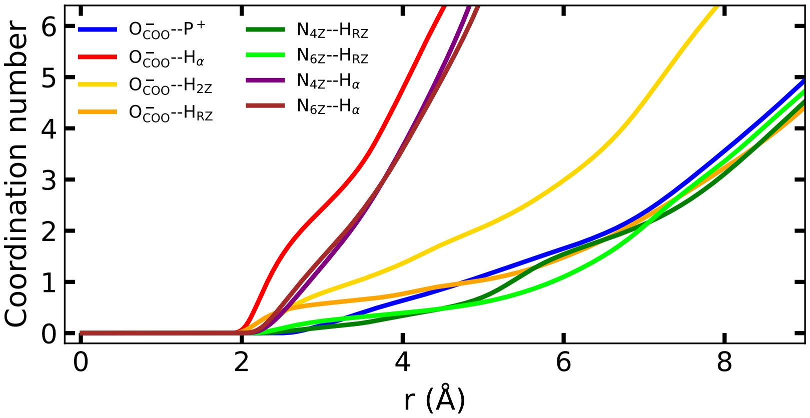

Figure S12 – Coordination number (CN) of (top) P^+, H_α and H_{RZ} around N_{4Z} and N_{6Z} of the $[TetrazC_1COO]^-$ anion, and O^- around H_{RZ} and H_{2Z} in $[P_{4,4,4,4}][TetrazC_1COO]$ at 343 K.

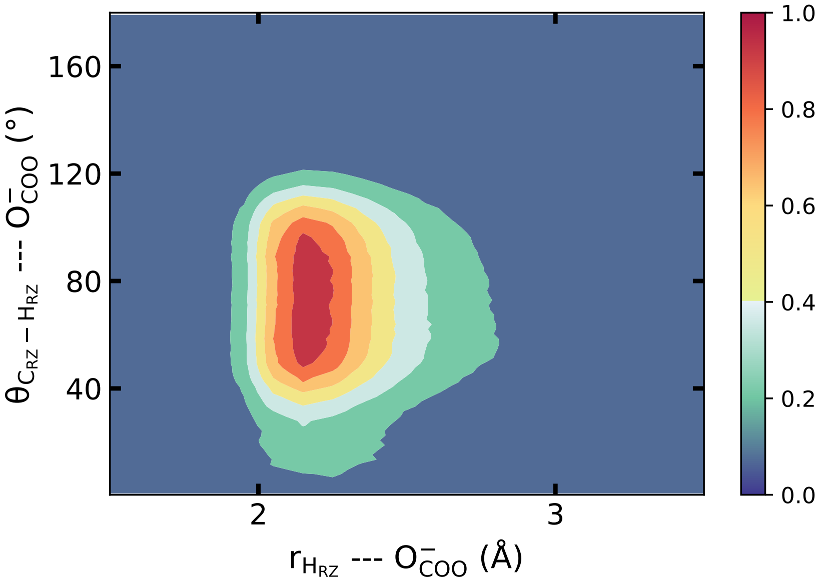

Figure S13 – CDF of the $C_{RZ}-H_{RZ}\cdots O^-_{COO}$ angle as a function of the RDF Angular Distribution Function (ADF) as a function of the RDF between the negatively chargedO^-_{COO} of the $[TetrazC_1COO]^-$ anion and the H_{RZ} of a neighbour anion in $[P_{4,4,4,4}][TetrazC_1COO]$ at 343 K.

SAXS data

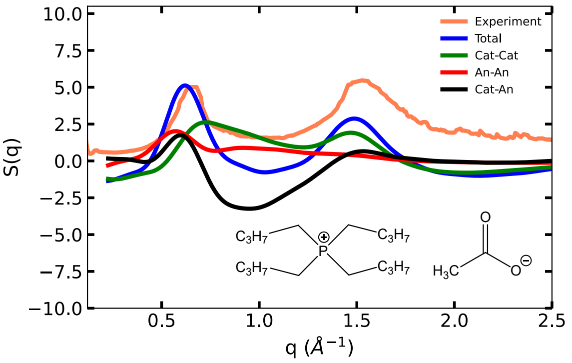

(a)

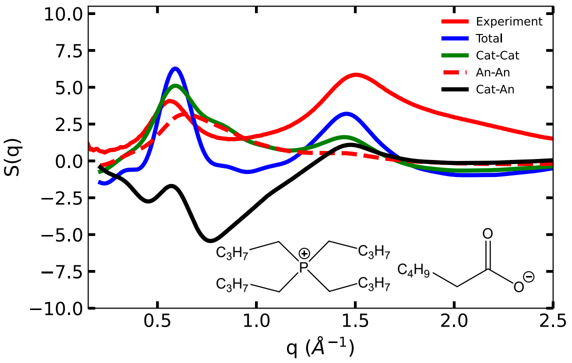

(b)

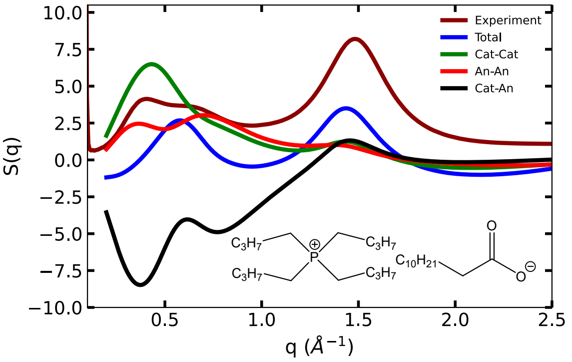

(c)

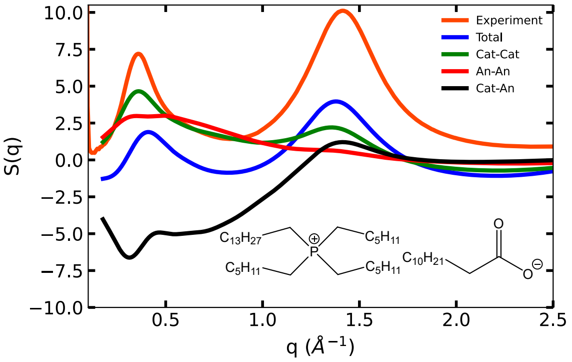

(d)

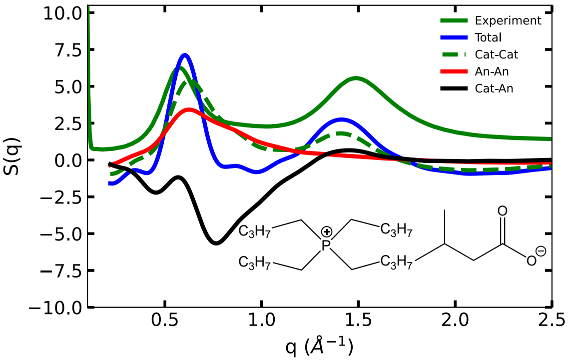

(e)

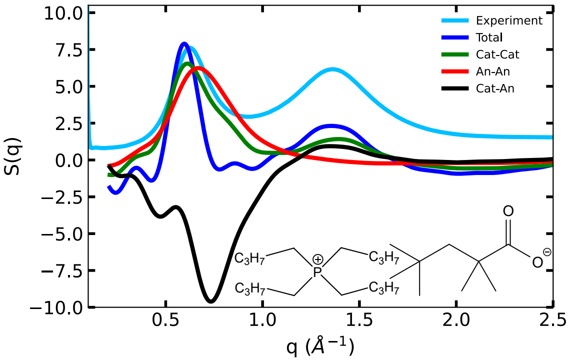

(f)

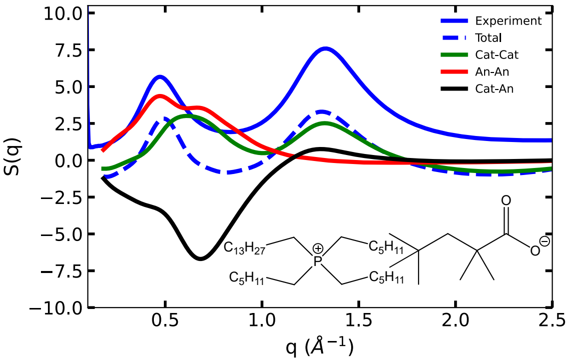

(g)

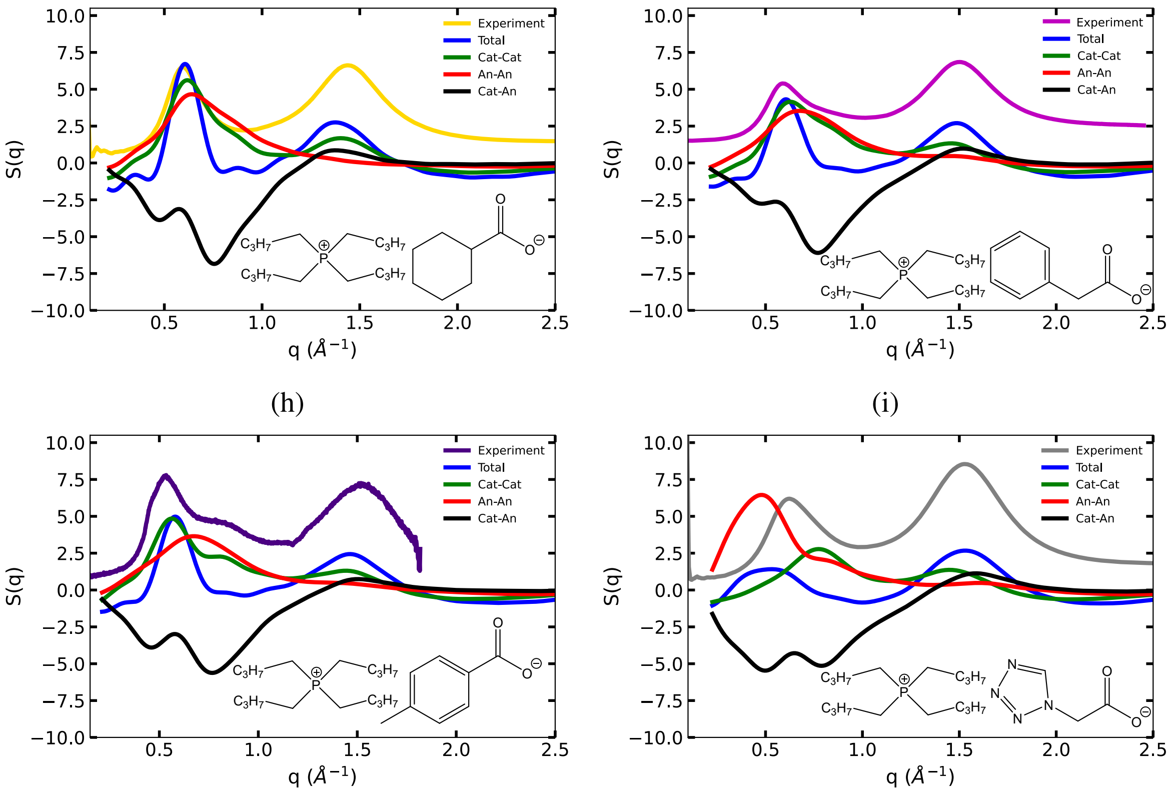

(h)

(i)

(j)

(k)

Figure S14 – Comparison of experimental with the total simulated S(q) as well as the partial S(q) for (a) [$P_{4,4,4,4}$][C_1COO], (b) [$P_{4,4,4,4}$][C_5COO], (c) [$P_{4,4,4,4}$][C_{11}COO], (d) [$P_{6,6,6,14}$][C_{11}COO], (e) [$P_{4,4,4,4}$][MeC_3COO], (f) [$P_{4,4,4,4}$][Me$_4C_4$COO], (g) [$P_{6,6,6,14}$][Me$_4C_4$COO], (h) [$P_{4,4,4,4}$][c−C_6COO], (i) [$P_{4,4,4,4}$][PhC_1COO], (j) [$P_{4,4,4,4}$][*p*−MeBzCOO] and (k) [$P_{4,4,4,4}$][TetrazC_1COO].

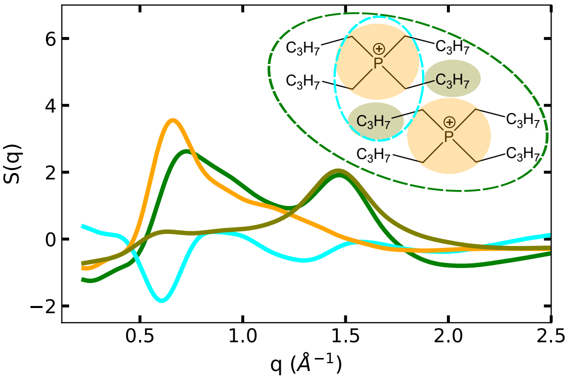
S(q)
6
4
2
0
−2
0.5
1.0
1.5
2.0
2.5
q (Å^{-1})
C_3H_7
P
⊕

(a)

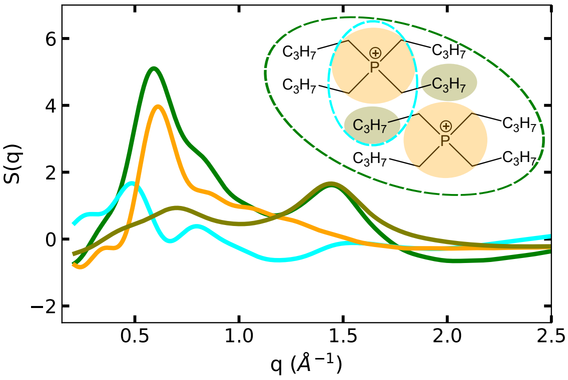
S(q)
6
4
2
0
−2
0.5
1.0
1.5
2.0
2.5
q (Å^{-1})
C_3H_7
P
⊕

(b)

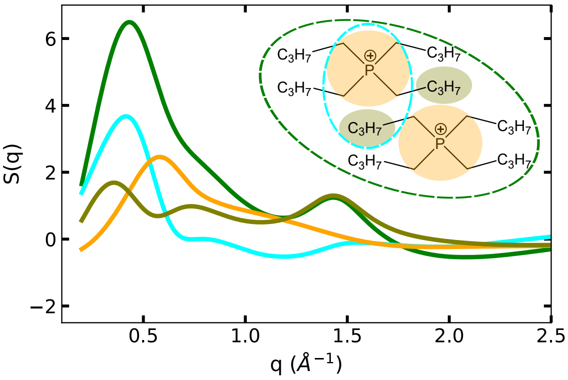
S(q)
6
4
2
0
−2
0.5
1.0
1.5
2.0
2.5
q (Å^{-1})
C_3H_7
P
⊕

(c)

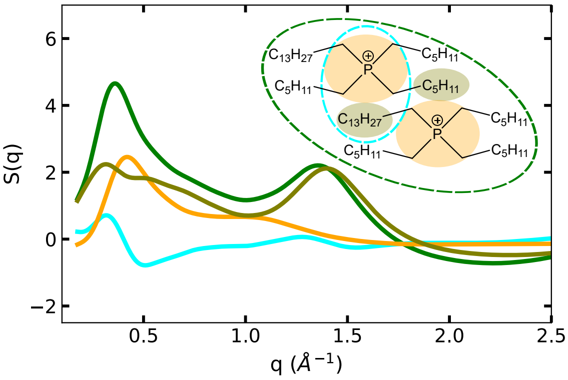
S(q)
6
4
2
0
−2
0.5
1.0
1.5
2.0
2.5
q (Å^{-1})
$C_{13}H_{27}$
C_5H_{11}
P
⊕

(d)

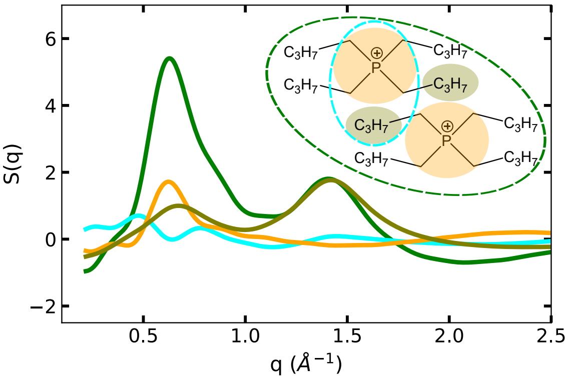
S(q)
6
4
2
0
−2
0.5
1.0
1.5
2.0
2.5
q (Å^{-1})
C_3H_7
P
⊕

(e)

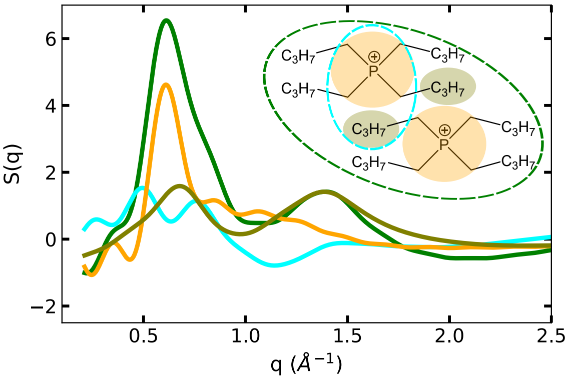
S(q)
6
4
2
0
−2
0.5
1.0
1.5
2.0
2.5
q (Å^{-1})
C_3H_7
P
⊕

(f)

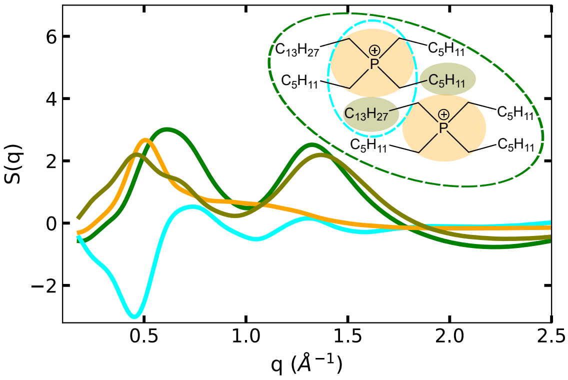
S(q)
6
4
2
0
−2
0.5
1.0
1.5
2.0
2.5
q (Å^{-1})
$C_{13}H_{27}$
C_5H_{11}
P
⊕

(g)

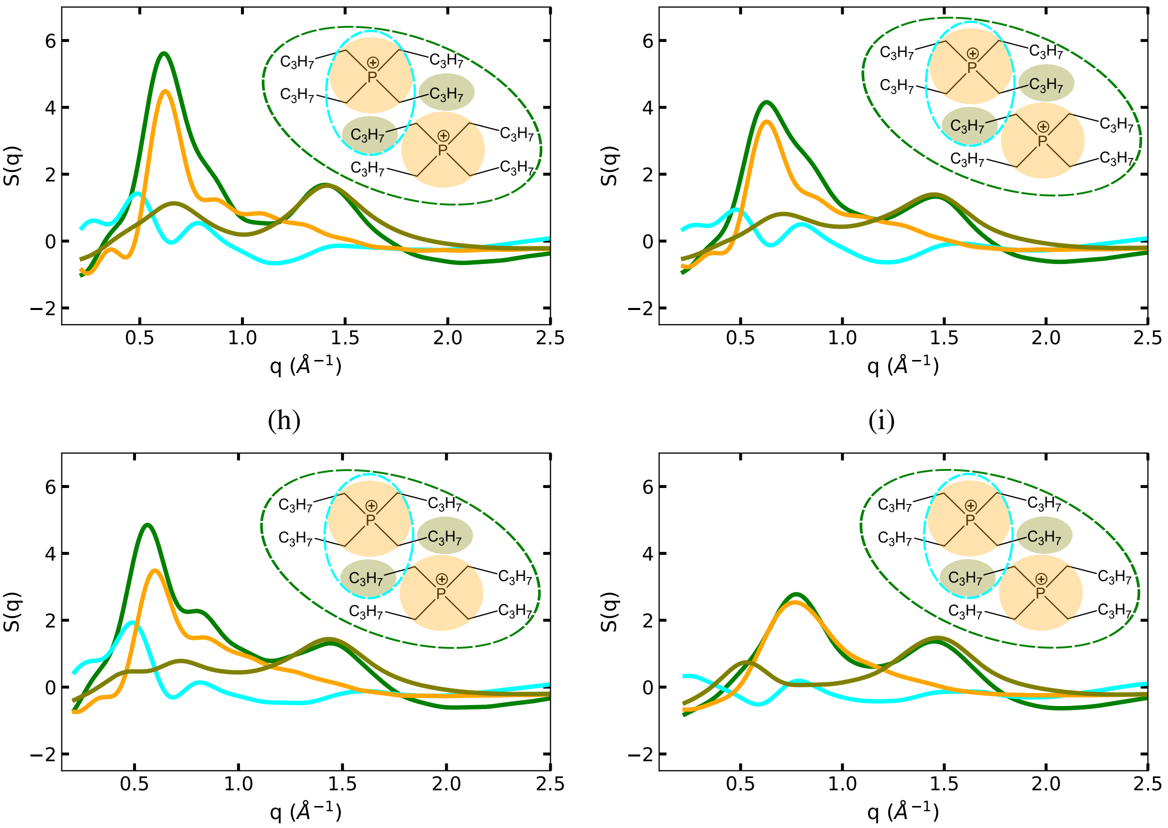

(h) (i)

(j) (k)

Figure S15 – 🟩 Cation-cation partial S(q) split into 🟦 head-tail, 🟨 head-head and 🟫 tail-tail components for (a) [$P_{4,4,4,4}$][C_1COO], (b) [$P_{4,4,4,4}$][C_5COO], (c) [$P_{4,4,4,4}$][C_{11}COO], (d) [$P_{6,6,6,14}$][C_{11}COO], (e) [$P_{4,4,4,4}$][MeC_3COO], (f) [$P_{4,4,4,4}$][Me$_4$C$_4$COO], (g) [$P_{6,6,6,14}$][Me$_4$C$_4$COO], (h) [$P_{4,4,4,4}$][c−C_6COO], (i) [$P_{4,4,4,4}$][PhC_1COO], (j) [$P_{4,4,4,4}$][*p*−MeBzCOO] and (k) [$P_{4,4,4,4}$][TetrazC_1COO].

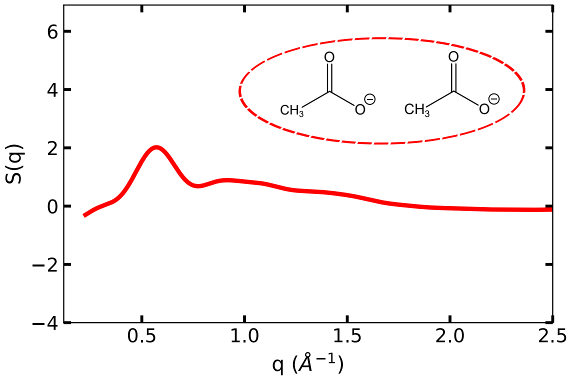
S(q)
q (Å^{-1})
6
4
2
0
−2
−4
0.5
1.0
1.5
2.0
2.5
CH$_3$
O
O$^{\ominus}$

(a)

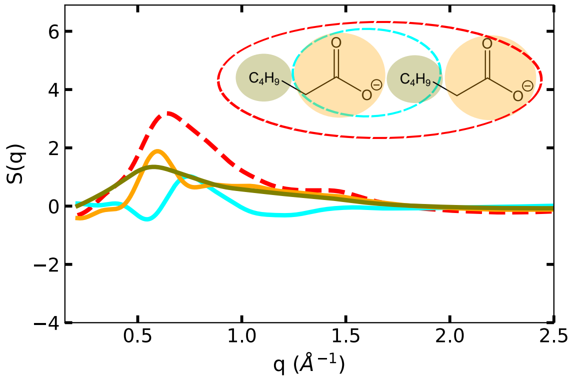
S(q)
q (Å^{-1})
6
4
2
0
−2
−4
0.5
1.0
1.5
2.0
2.5
C$_4$H$_9$
O
O$^{\ominus}$

(b)

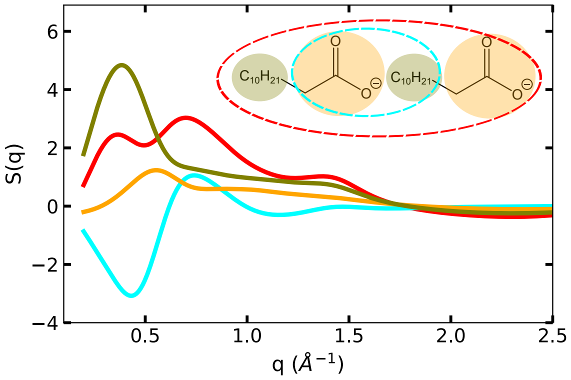
S(q)
q (Å^{-1})
6
4
2
0
−2
−4
0.5
1.0
1.5
2.0
2.5
C$_{10}$H$_{21}$
O
O$^{\ominus}$

(c)

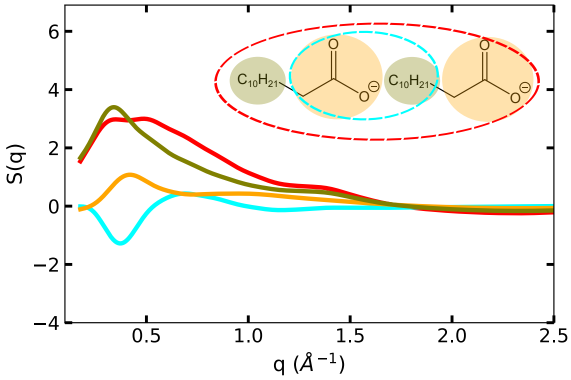
S(q)
q (Å^{-1})
6
4
2
0
−2
−4
0.5
1.0
1.5
2.0
2.5
C$_{10}$H$_{21}$
O
O$^{\ominus}$

(d)

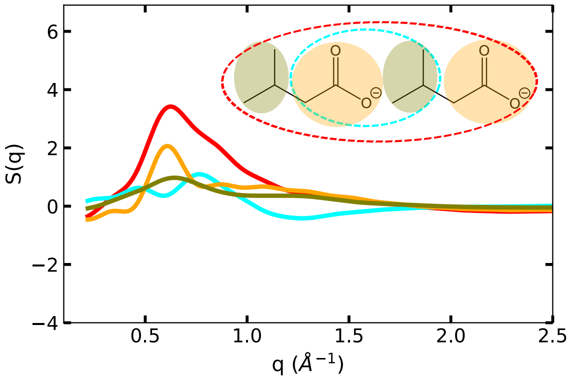
S(q)
q (Å^{-1})
6
4
2
0
−2
−4
0.5
1.0
1.5
2.0
2.5
O
O$^{\ominus}$

(e)

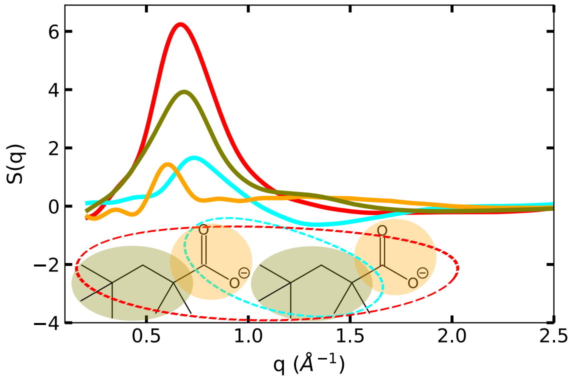
S(q)
q (Å^{-1})
6
4
2
0
−2
−4
0.5
1.0
1.5
2.0
2.5
O
O$^{\ominus}$

(f)

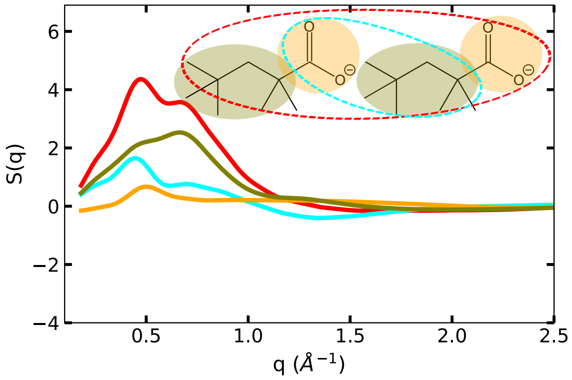
S(q)
q (Å^{-1})
6
4
2
0
−2
−4
0.5
1.0
1.5
2.0
2.5
O
O$^{\ominus}$

(g)

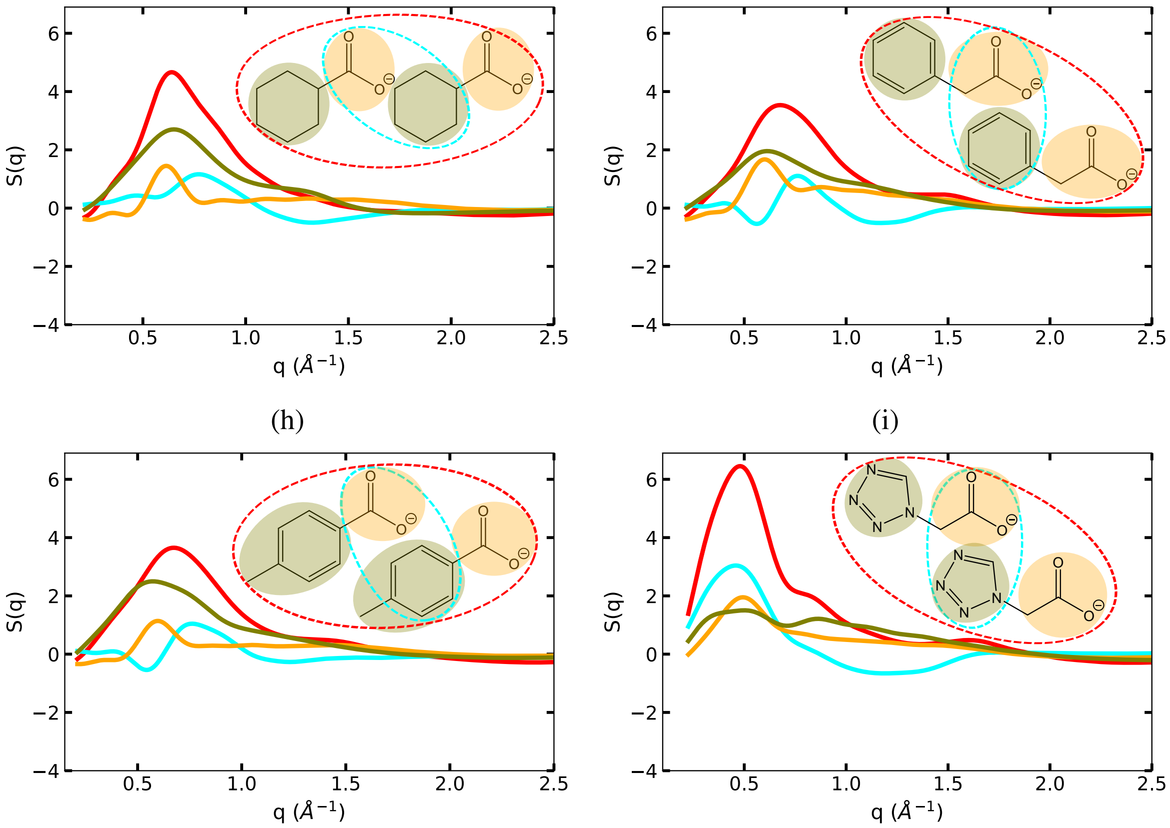

(h) (i)

(j) (k)

Figure S16 – 🟥 Anion-anion partial S(q) split into 🟦 head-tail, 🟨 head-head and 🟩 tail-tail or ring-ring components as indicated in the graphs for (a) $[P_{4,4,4,4}][C_1COO]$, (b) $[P_{4,4,4,4}][C_5COO]$, (c) $[P_{4,4,4,4}][C_{11}COO]$, (d) $[P_{6,6,6,14}][C_{11}COO]$, (e) $[P_{4,4,4,4}][MeC_3COO]$, (f) $[P_{4,4,4,4}][Me_4C_4COO]$, (g) $[P_{6,6,6,14}][Me_4C_4COO]$, (h) $[P_{4,4,4,4}][c{-}C_6COO]$, (i) $[P_{4,4,4,4}][PhC_1COO]$, (j) $[P_{4,4,4,4}][p{-}MeBzCOO]$ and (k) $[P_{4,4,4,4}][TetrazC_1COO]$.

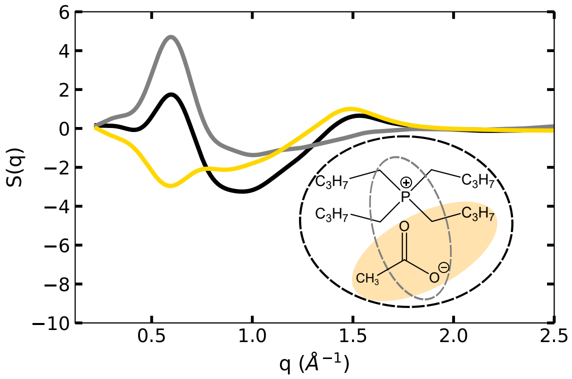
6
4
2
0
−2
−4
−6
−8
−10
S(q)
0.5
1.0
1.5
2.0
2.5
q (Å^{-1})
C$_3$H$_7$
C$_3$H$_7$
C$_3$H$_7$
C$_3$H$_7$
P
O
CH$_3$
O

(a)

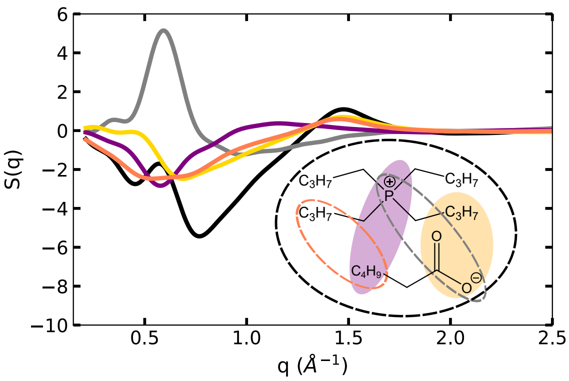
6
4
2
0
−2
−4
−6
−8
−10
S(q)
0.5
1.0
1.5
2.0
2.5
q (Å^{-1})
C$_3$H$_7$
C$_3$H$_7$
C$_3$H$_7$
C$_3$H$_7$
P
O
C$_4$H$_9$
O

(b)

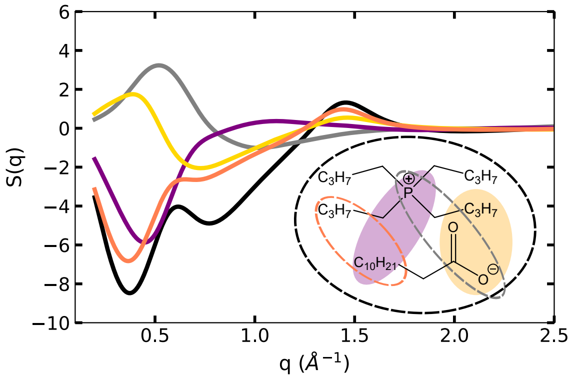
6
4
2
0
−2
−4
−6
−8
−10
S(q)
0.5
1.0
1.5
2.0
2.5
q (Å^{-1})
C$_3$H$_7$
C$_3$H$_7$
C$_3$H$_7$
C$_3$H$_7$
P
O
C$_{10}$H$_{21}$
O

(c)

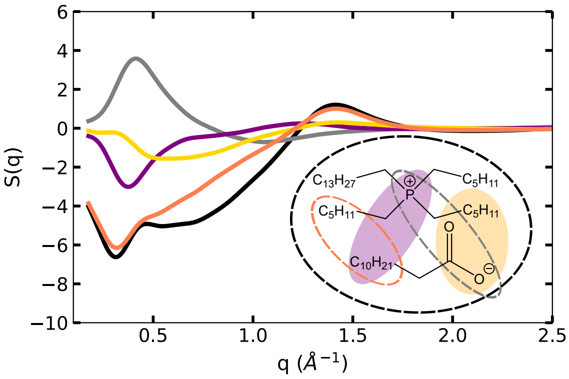
6
4
2
0
−2
−4
−6
−8
−10
S(q)
0.5
1.0
1.5
2.0
2.5
q (Å^{-1})
C$_{13}$H$_{27}$
C$_5$H$_{11}$
C$_5$H$_{11}$
C$_5$H$_{11}$
P
O
C$_{10}$H$_{21}$
O

(d)

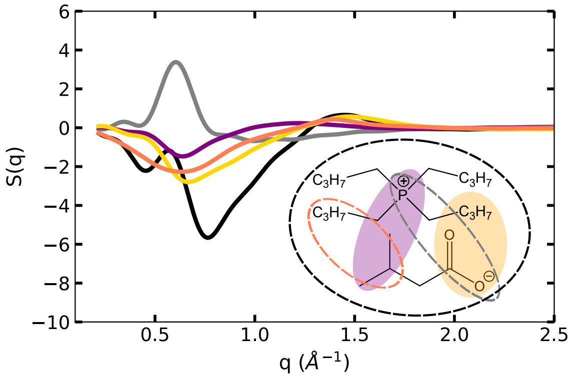
6
4
2
0
−2
−4
−6
−8
−10
S(q)
0.5
1.0
1.5
2.0
2.5
q (Å^{-1})
C$_3$H$_7$
C$_3$H$_7$
C$_3$H$_7$
C$_3$H$_7$
P
O
O

(e)

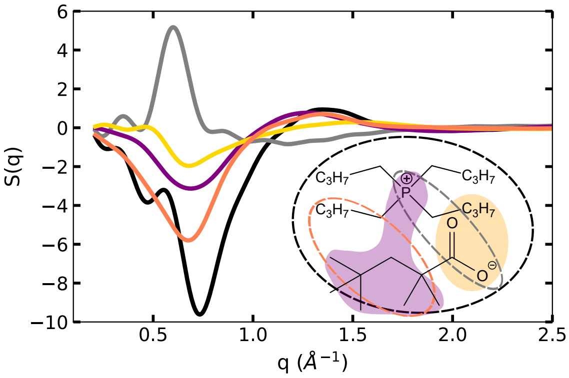
6
4
2
0
−2
−4
−6
−8
−10
S(q)
0.5
1.0
1.5
2.0
2.5
q (Å^{-1})
C$_3$H$_7$
C$_3$H$_7$
C$_3$H$_7$
C$_3$H$_7$
P
O
O

(f)

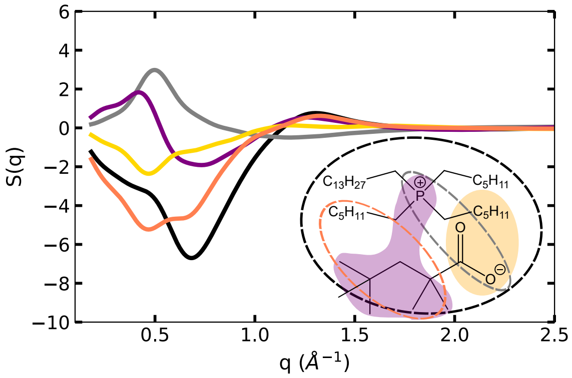
6
4
2
0
−2
−4
−6
−8
−10
S(q)
0.5
1.0
1.5
2.0
2.5
q (Å^{-1})
C$_{13}$H$_{27}$
C$_5$H$_{11}$
C$_5$H$_{11}$
C$_5$H$_{11}$
P
O
O

(g)

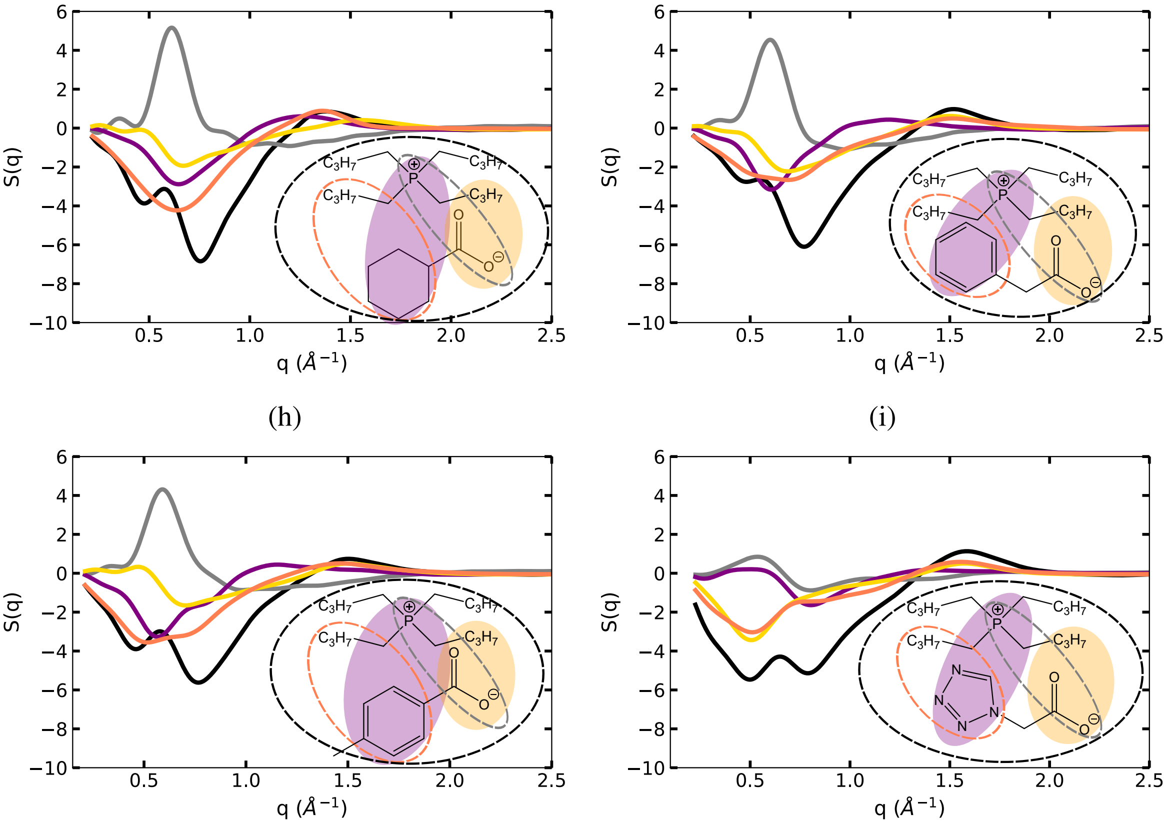

(h)

(i)

(j)

(k)

Figure S17 – ■ Cation-anion partial S(q) split into ■ cation head-anion head, ■ cation head-anion ring/tail, ■ cation tail-anion head and ■ cation tail-anion ring/tail components for (a) [$P_{4,4,4,4}$][C_1COO], (b) [$P_{4,4,4,4}$][C_5COO], (c) [$P_{4,4,4,4}$][C_{11}COO], (d) [$P_{6,6,6,14}$][C_{11}COO], (e) [$P_{4,4,4,4}$][MeC_3COO], (f) [$P_{4,4,4,4}$][Me$_4C_4$COO], (g) [$P_{6,6,6,14}$][Me$_4C_4$COO], (h) [$P_{4,4,4,4}$][c−C_6COO], (i) [$P_{4,4,4,4}$][PhC_1COO], (j) [$P_{4,4,4,4}$][*p*−MeBzCOO] and (k) [$P_{4,4,4,4}$][TetrazC_1COO].

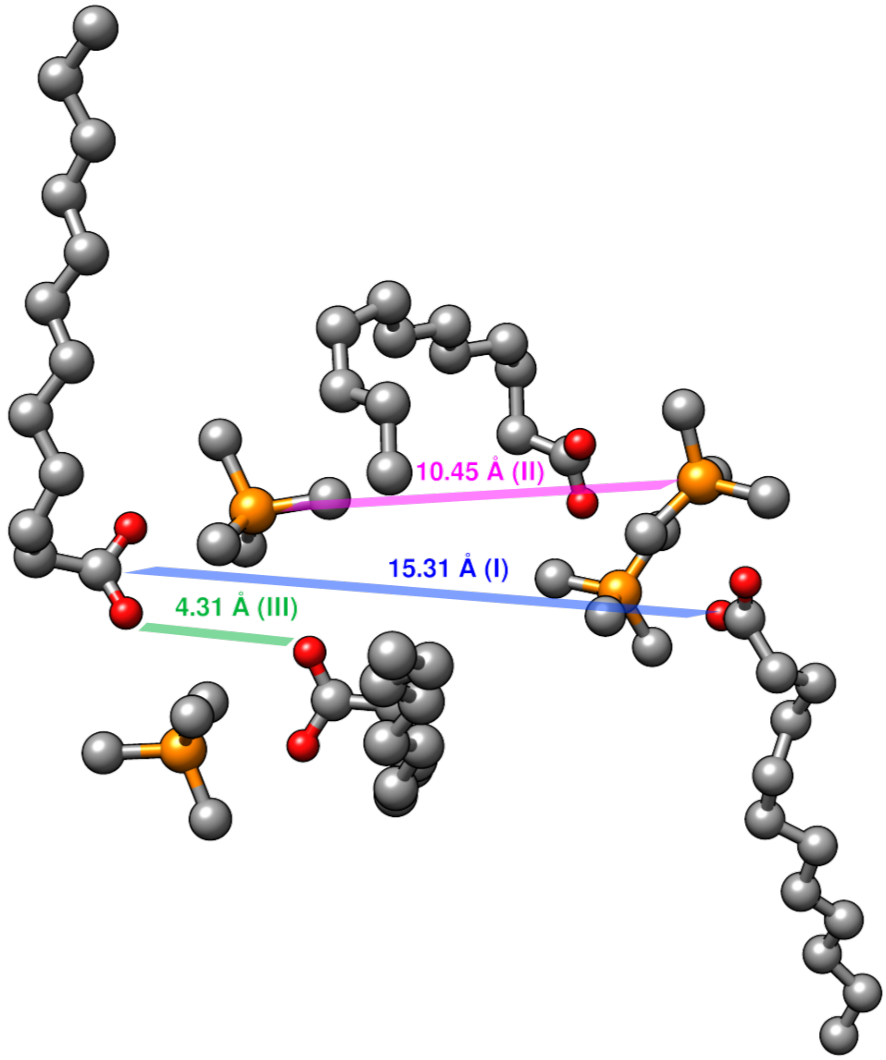

Figure S18 – Snapshot from the $[P_{4,4,4,4}][C_{11}COO]$ molecular simulation box illustrating the three different domains and their size observed by SAXS experiments.

References

(1) Avila, J.; Lepre, L. F.; Santini, C. C.; Tiano, M.; Denis-Quanquin, S.; Szeto, K. C.; Padua, A. A. H.; Gomes, M. C. High-Performance Porous Ionic Liquids for Low-Pressure CO2 Capture. *Angew. Chem. Int. Ed.* **2021**, *60*, 12876–12882.

(2) Jacquemin, J.; Ge, R.; Nancarrow, P.; Rooney, D. W.; Costa Gomes, M. F.; Pádua, A. A. H.; Hardacre, C. Prediction of Ionic Liquid Properties. I. Volumetric Properties as a Function of Temperature at 0.1 MPa. *J. Chem. Eng. Data* **2008**, *53*, 716–726.

(3) Zhou, Q.; Song, Y.; Yu, Y.; He, H.; Zhang, S. Density and Excess Molar Volume for Binary Mixtures of Naphthenic Acid Ionic Liquids and Ethanol. *J. Chem. Eng. Data* **2010**, *55*, 1105–1108.

(4) Zhao, N.; Menegolla, H. B.; Degirmenci, V.; Wagner, Z.; Bendová, M.; Jacquemin, J. Group Contribution Method for Evaluation of Volumetric Properties of Ionic Liquids Using Experimental Data Recommended by Mathematical Gnostics. *Ind. Eng. Chem. Res.* **2017**, *56*, 6827–6840.

(5) Deng, Y.; Morrissey, S.; Gathergood, N.; Delort, A.-M.; Husson, P.; Costa Gomes, M. F. The Presence of Functional Groups Key for Biodegradation in Ionic Liquids: Effect on Gas Solubility. *ChemSusChem* **2010**, *3*, 377–385.

(6) Fillion, J. J.; Xia, H.; Desilva, M. A.; Quiroz-Guzman, M.; Brennecke, J. F. Phase Transitions, Decomposition Temperatures, Viscosities, and Densities of Phosphonium, Ammonium, and Imidazolium Ionic Liquids with Aprotic Heterocyclic Anions. *J. Chem. Eng. Data* **2016**, *61*, 2897–2914.

(7) Pena, C. A.; Soto, A.; King, A. W. T.; Rodríguez, H. Improved Reactivity of Cellulose via Its Crystallinity Reduction by Nondissolving Pretreatment with an Ionic Liquid. *ACS Sustain. Chem. Eng.* **2019**, *7*, 9164–9171.